Boolean algebra of two-dimensional continua with arbitrarily complex topology

Article *in* Mathematics of Computation · May 2020

DOI: 10.1090/mcom/3539

CITATIONS
3

READS
328

2 authors:

Qinghai Zhang
Zhejiang University
31 PUBLICATIONS **372** CITATIONS
SEE PROFILE

Zhixuan Li
Zhejiang University
3 PUBLICATIONS **3** CITATIONS
SEE PROFILE

MATHEMATICS OF COMPUTATION
Volume 00, Number 0, Pages 000–000
S 0025-5718(XX)0000-0

BOOLEAN ALGEBRA OF TWO-DIMENSIONAL CONTINUA WITH ARBITRARILY COMPLEX TOPOLOGY

QINGHAI ZHANG AND ZHIXUAN LI

Abstract. We propose a mathematical model for two-dimensional continua in order to establish a solid theoretical foundation for the study of their complex topology, large geometric deformations, and topological changes such as merging in the context of multiphase flows. Our modeling space, named the Yin space, consists of regular open semianalytic sets with bounded boundaries, and is further equipped with constructive and algebraic definitions of Boolean operations. Major distinguishing features of our model include (a) topological information of fluids such as Betti numbers can be easily extracted in constant time, (b) topological changes of fluids are captured by non-manifold points on fluid boundaries, and (c) Boolean operations on fluids correctly handle all degenerate cases and apply to arbitrarily complex topologies, yet they are simple and efficient in that they only involve determining the relative position of a point to a Jordan curve and intersecting a number of curve segments.

1. Introduction

Physically meaningful regions in the sense of homogeneous continua are ubiquitous, and their modeling is of fundamental significance in innumerable applications of science and engineering. Traditionally, the modeling of two- and three-dimensional physical regions is the main subject of a mature research field called solid modeling [29, 35]. In comparison, modeling of fluids have always been avoided in the field of multiphase flows. However, rapid advancements in the science of multiphase flows have been calling for such a model so that complex phenomena such as those involving topological changes of fluids can be studied rigorously.

In this paper, we aim to answer this need by introducing the notion of *fluid modeling* in multiphase flows, analogous to solid modeling in computer-aided design (CAD). We propose a topological space for fluid modeling and further equip this space with natural algebraic structures in order to extract essential topological information and to perform simple and efficient Boolean operations.

In Sections 1.1, 1.2, and 1.3, we motivate different aspects of fluid modeling and review previous efforts and relevant results. We then list in Section 1.4 a number of questions as the more detailed targets of this work.

1.1. **Solid modeling.** What distinguishes solid modeling from similar disciplines such as computer graphics is its emphasis on *physical fidelity*, as evident in its underlying mathematical and computational principles. This emphasis is natural:

2010 *Mathematics Subject Classification.* 65D18,76T99.

This work was supported by a grant (approval #11871429) from the National Natural Science Foundation of China.

driven by the design, analysis, and manufacture of engineering systems, solid modeling must support the representation, visualization, exchange, interrogation, and creation of physical objects in CAD.

One common approach of solid modeling relies on point-set topology. The classical modeling space proposed by Requicha and colleagues [28, 31, 30] consists of *r-sets*, which are bounded, closed, regular semianalytic sets in Euclidean spaces. The regularity condition captures in solid continua the absence of low-dimensional features such as isolated gaps and points, and the semianalytic condition postulates that the boundary of a solid be locally well behaved; see Section 3.1 for more details.

The other common approach in solid modeling is *combinatorial*, in the sense of *cell complexes* in algebraic topology [22] [34]. Complex objects are viewed in terms of primitive building blocks called *cells*, thus it is not the constituting cells but their combinatorial informations that describe the physical object. Take simplicial complexes for example, a *k-cell* is a k-simplex in the Euclidean space $\mathbb{R}^k$, and many cells of different dimensions are glued together to form an n-dimensional simplicial complex by requiring that any adjacent pair of k-cells be attached to each other along a $(k-1)$-cell for each $k = 1, \ldots, n$. The adjacency of k-cells is encoded in the *kth boundary operator* ∂_k, which maps each k-cell to an element in the $(k-1)$-*chain* C_{k-1}, a group of formal sums of $(k-1)$-cells. If we concatenate the chain groups with the boundary operators, we obtain a *chain complex*,

$$C_n \xrightarrow{\partial_n} \cdots \xrightarrow{\partial_{k+1}} C_k \xrightarrow{\partial_k} \cdots \xrightarrow{\partial_1} C_0 \ , \tag{1.1}$$

where each boundary operator is a group homomorphism and any two adjacent operators concatenate to the zero map. This chain complex is all we need for mathematical modeling and computer representation of any n-dimensional solid! As a prominent advantage, key topological quantities, such as the number of connected components and the number of holes, can be systematically computed from the chain complex. The cost of this computation, however, can be substantial [15].

Thanks to the fact that any r-set can be represented by a simplicial complex as accurately as one wishes, the point-set approach and the combinatorial approach are seamlessly consistent [30]. Thus we can use these two models interchangeably. This consistency also forces an n-dimensional r-set to be closed; otherwise a boundary operator in (1.1) may have a range outside of the chain complex.

1.2. **Fluid modeling and interface tracking (IT) in multiphase flows.** In dramatic comparison to the aforementioned research on solid modeling, efforts on geometric modeling of fluids are rare: mathematical models and computer algorithms have been deliberately designed such that *geometric* modeling of fluids is avoided in numerically simulating multiphase flows.

In the volume-of-fluid (VOF) method [12], a deforming fluid phase M is represented by a *color function* $f(\mathbf{x}, t)$,

$$f(\mathbf{x}, t) := \begin{cases} 1 & \text{if there is } \mathsf{M} \text{ at } (\mathbf{x},\text{t}); \\ 0 & \text{otherwise,} \end{cases} \tag{1.2}$$

then the area occupied by M at time t is a point set

$$\mathcal{M}(t) := \{\mathbf{x} : f(\mathbf{x}, t) = 1\}. \tag{1.3}$$

Either the scalar conservation law

$$\frac{\partial f}{\partial t} + \nabla \cdot (f\mathbf{u}) = 0 \tag{1.4}$$

or the advection equation

$$\frac{\partial f}{\partial t} + \mathbf{u} \cdot \nabla f = 0 \tag{1.5}$$

is solved to recover the boundary of $\mathcal{M}$ at subsequent time instants. In the level-set method [25], the boundary of a fluid phase is represented as the zero isocontour of a signed distance function ϕ, and once again the region of the fluid phase is recovered by numerically solving either (1.4) or (1.5) on ϕ. In the front tracking method [40], the boundary of a fluid phase is represented by connected Lagrangian markers; tracking the fluid phase is then reduced to tracking these markers via numerically solving ordinary differential equations. In all of these IT methods, geometric problems in deforming fluids with sharp interfaces are converted to numerically solving differential equations. With topological information discarded, this conversion largely reduces the complexity of IT both theoretically and computationally; this is a main reason for successes of the aforementioned IT methods. During the past forty years, these IT methods have been extremely valuable in studying multiphase flows.

As the science of multiphase flows moves towards more and more complex phenomena, higher and higher expectations are imposed on IT. First, the wider and wider spectrum of relevant time scales and length scales in mainstream problems demands that IT methods be more and more accurate and efficient. Second, the tight coupling of interface to ambient fluids necessitates accurate estimation of derived geometric quantities such as curvature and unit normal/tangential vectors. Third, topological changes of a fluid phase such as merging exhibit distinct behaviors for different regimes of the Weber number and other impact parameters [27], hence it is not enough to handle topological changes solely from the interface locus and the velocity field. For these problems, an IT method should also take as its input a policy that describes how the interface shall evolve at the branching time and place of topological changes.

Despite their tremendous successes, current IT methods have a number of limitations in answering the aforementioned challenges of multiphase flows. First, most methods are at best second-order accurate [43]. Second, the IT errors put an upper limit on the accuracy of estimating curvature and unit vectors. It is shown in [47] that, for a second-order method, its error of curvature estimation is proportional to $\sqrt{\epsilon_p}$ where ϵ_p denotes a norm of IT errors. In other words, the number of accurate digits one gets in curvature estimation is at best half of that in the IT results. Third, the avoidance of geometric modeling of fluids renders it highly difficult to treat topological changes rigorously. When merging and separation happen, front-tracking methods have to resort to "surgical" operations that are short of theoretical justification. VOF methods and level-set methods have no special procedures for topological changes; this is often advertised as an advantage. However, by using this "automatic" treatment, an application scientist has *no control* over the evolution of an interface that undergoes topological changes: the evolution is determined not by the physics, but by particularities of numerical algorithms [43, 48]. Clearly, this disadvantage is a consequence of avoiding the geometric and topological modeling of fluids.

In this work, we aim to *establish a theoretical foundation for fluid modeling*. To prevent reinventing the wheel, we have tried to utilize the wealth of solid modeling, but found that none of the two main approaches in Section 1.1 is adequate for fluid modeling. Topology computing based on cell complexes involves much machinery, yet its efficiency may not be acceptable; nor are the r-sets suitable for fluid modeling. First, the requirement of r-sets being closed is not amenable to numerical analysis of IT methods [43]. Second, topological changes create on the fluid boundary a special type of non-manifold points, such as the q points in Figure 1, which cause non-uniqueness of boundary representations, c.f. Figure 5. This non-uniqueness degrades isomorphisms to homomorphisms in the association of algebraic structures with elements in the topological modeling space. Third, r-sets can be modified to yield a new Boolean algebra whose implementation is much simpler and more efficient.

1.3. **Boolean operations.** The operations to be performed on the modeling space are an indispensable part of the modeling process; after all, a major purpose of modeling is to answer questions on the objects being modeled. Hence theoretically a modeling space is shaped by primary cases of queries. Computationally, these operations should be defined algebraically and constructively so that they furnish realizable algorithms that finish in reasonable time.

We are interested in Boolean operations on physically meaningful regions with arbitrarily complex topologies. This interest follows naturally from the motivations in Section 1.2. First, we have shown that algorithms for clipping splinegons with a linear polygon can improve the IT accuracy by many orders of magnitudes [48]. Second, for coupling an IT method to an Eulerian main flow solver, regions occupied by the fluid inside fixed control volumes are needed to define averaged values and to construct stencils for approximating spatial operators with linear combinations of these averaged values. Third, in handling topological changes, the emerging time and sites of non-manifold points need to be detected on the fluid boundary before we are able to decide how to evolve it. This detecting problem requires calculating intersections of multiple regions inside a single control volume.

Boolean operations on polygons are an active and intense research topic in many related fields such as computational geometry, computer graphics, CAD, and geographic information system (GIS). In particular, physically meaningful regions in GIS such as parks, roads, and lakes are represented by polygons and their Boolean operations are essential for extracting information and answering queries. Consequently, there exist numerous papers on this topic; see, e.g., [38, 18, 41, 10, 24, 19, 7, 36, 21] and references therein. However, many current algorithms are subject to strong restrictions on operand polygons such as convexity, simple-connectedness, and no self-intersections. In addition, most algorithms fail for degenerate cases such as a vertex of a polygon being on the edge of the other polygon; these degenerate scenarios, nonetheless, are at the core of characterizing and treating topological changes. Therefore, current Boolean algorithms are not suitable for fluid modeling.

As another main reason for their lack of applicability in multiphase flows, very few of current Boolean algorithms have a solid mathematical foundation, and those that do have other notable drawbacks. For example, Boolean algorithms based on cell complexes [26, 32] seem to be inefficient for complex topologies. Those based on Nef polyhedra [23, 3, 11] have an elegant theoretical foundation and is applicable to arbitrarily complex topologies, but they appear as an overkill for fluid

modeling in that many elements in the modeling space of Nef polyhedra do not have counterparts in multiphase flows. In addition, the corresponding algorithms and data structures are complicated and difficult to implement. For both types of algorithms, computing the topological information such as Betti numbers would be very time-consuming.

1.4. **Motivations and contributions of this work.** Methods that couple elementary concepts or tools from multiple disciplines often perform surprisingly well. For fluid-structure interactions, a recent approach called isogeometric analysis [6, 1] has been increasingly popular, and much of its success is due to the integration of finite element methods with highly accurate (and sometimes exact) solid modeling in CAD. In our previous work, we have adopted a similar guiding principle to integrate IT with a topological space for fluid modeling [49]. The resulting generic framework, called MARS, furnishes new tools for analyzing current IT methods [43] and leads to a new IT method and a new curvature-estimation algorithm that are more accurate than current methods by many orders of magnitudes [47, 48].

In recognition of the potentially large benefits of integrating fluid modeling with multiphase flows and in view of the discussions in previous subsections, we list a number of questions as the driving forces behind this work.

(Q-1) Can we propose a generic topological space that appropriately models physically meaningful regions across multiple research fields such as solid modeling, GIS, and multiphase flows?
(Q-2) Can we find a simple representation scheme for elements in the modeling space to facilitate geometric and topological queries?
(Q-3) Can we design simple and efficient Boolean operations that correctly handle all degenerate cases?
(Q-4) In particular, can we provide theoretical underpinning and algorithmic support for handling topological changes of moving regions?
(Q-5) Meanwhile, can we extract topological information such as Betti numbers with optimal complexity?

In this paper, we provide positive answers to all of the above questions. (Q-1) is answered in Section 3, where physically meaningful regions are modeled by a topological space, called the Yin space, which consists of regular open semianalytic sets with bounded boundaries. These conditions capture fluid features that are commonly relevant in multiphase flows, solid modeling, and GIS. Furthermore, Yin sets are defined in terms of computable *mathematical* properties and are thus independent of any particular representation or individual application. As such, this modeling space serves as a bridge between multiphase flows and the other fields that emphasize geometry and topology. As our answer to (Q-2), each Yin set can be uniquely expressed as the result of finite Boolean operations on interiors of oriented Jordan curves. This uniqueness leads to an isomorphism from the Yin space into the Jordan space, a collection of certain posets of oriented Jordan curves, and this isomorphism reduces Boolean algebra on the two-dimensional Yin space to one-dimensional routines in the Jordan space, namely locating a point relative to a simple polygon and finding intersections of curve segments. This is our answer to (Q-3); see Section 4.

In addressing (Q-4), we pay special attentions to issues related to non-manifold points on the fluid boundary, such as characterizing topological changes with improper intersections of curves and dividing closed curves at these improper intersections to ensure correctness of Boolean operations. However, we emphasize that, in both our theory and our algorithms, non-manifold points of topological changes are treated not as an anomaly, but as a natural consequence of capturing the physical meaningfulness of fluids with the mathematical conditions that constitute the notion of Yin sets. This is a major advantage of the Yin sets over the r-sets.

As another prominent feature of our theory, the number of connected components in any bounded Yin set is simply the number of positively oriented Jordan curves in its boundary representation, and the number of holes in a component is the number of negatively oriented Jordan curves in the boundary representation of that component. Since these numbers are returned in $O(1)$ time, our answer to (Q-5) is of optimal complexity.

The rest of this paper is organized as follows. In Section 2, we introduce prerequisites and notation. In Section 3, we propose Yin sets as our fluid modeling space and study its topological properties. In Section 4, we design Boolean operations on the Yin space in a way so that corresponding algorithms can be implemented by straightforward orchestration of these definitions. In Section 5, we give algorithmic details on implementing the Boolean algebra of Yin sets. Utilizing the Bentley-Ottmann paradigm of plane sweeping [2] in calculating intersections of curve segments, our implementation of the Boolean operations is close to optimal complexity. A number of fun tests are given in Figure 13 to illustrate the Boolean algorithm. In Section 5.5, we approach interface tracking of multiphase flows from the viewpoint of the actions of continuous flow maps upon Yin sets. Results of numerical tests demonstrate that interface tracking based on the proposed Boolean algorithms preserves complex topologies of the fluid if the flow map is homeomorphic. Finally, we draw the conclusion and discuss several research prospects in Section 6.

2. Preliminaries

In this section we collect relevant definitions and theorems that form the *algebraic* foundation of this work. Some notations introduced here will be repeatedly used in subsequent sections.

2.1. **Partially ordered sets.** The Cartesian product of a nonempty set $\mathcal{A}$ with itself n times is denoted by $\mathcal{A}^n$; in particular, $\mathcal{A}^0 = \{\emptyset\}$. An *$n$-ary relation on $\mathcal{A}$* is a subset of $\mathcal{A}^n$; if $n = 2$ it is called a *binary relation*. A given binary relation "$\sim$" on a set $\mathcal{A}$ is said to be an *equivalence relation* if and only if it is *reflexive* ($a \sim a$), *symmetric* ($a \sim b \ \Rightarrow \ b \sim a$), and *transitive* ($a \sim b, b \sim c \ \Rightarrow \ a \sim c$) for all $a, b, c \in \mathcal{A}$. A binary relation "$\leq$" defined on a set $\mathcal{A}$ is a *partial order* on $\mathcal{A}$ if and only if it is reflexive ($a \leq a$), *antisymmetric* ($a \leq b, b \leq a \ \Rightarrow \ b = a$), and transitive ($a \leq b, b \leq c \ \Rightarrow \ a \leq c$) for all $a, b, c \in \mathcal{A}$.

A nonempty set $\mathcal{A}$ with a partial order $\leq$ on it is called a *partially ordered set*, or more briefly a *poset*. Two elements $a, b \in \mathcal{A}$ are *comparable* if either $a \leq b$ or $b \leq a$; otherwise a and b are *incomparable*. If all $a, b \in \mathcal{A}$ are comparable by $\leq$, then "$\leq$" is a *total order* on $\mathcal{A}$ and $\mathcal{A}$ is a *chain* or linearly-ordered set. For examples, $\mathbb{R}$ with the usual order of real numbers is a chain; the *power set* of $\mathcal{A}$, i.e. the set of all

subsets of $\mathcal{A}$, with the subset relation "$\subseteq$" is a poset but not a chain. The notation $a \geq b$ means $b \leq a$, and $a < b$ means both $a \leq b$ and $a \neq b$.

Definition 2.1 (Covering relation)**.** Let $\mathcal{A}$ denote a poset and $a, b \in \mathcal{A}$. We say b *covers* a and write $a \prec b$ or $b \succ a$ if and only if $a < b$ and no element $c \in \mathcal{A}$ satisfy $a < c < b$.

Most concepts on the ordering of $\mathbb{R}$ make sense for posets. Let $\mathcal{A}$ be a subset of a poset $\mathcal{P}$. An element $p \in \mathcal{P}$ is an *upper bound* of $\mathcal{A}$ if $a \leq p$ for all $a \in \mathcal{A}$. $p \in \mathcal{P}$ is the *least upper bound* of $\mathcal{A}$, or *supremum* of $\mathcal{A}$ ($\sup \mathcal{A}$) if p is an upper bound of $\mathcal{A}$, and $p \leq b$ for any upper bound b of $\mathcal{A}$. Similarly we can define the concepts of a *lower bound* and the *greatest lower bound* of $\mathcal{A}$ or the *infimum* of $\mathcal{A}$ ($\inf \mathcal{A}$).

Definition 2.2 (Lattice as a poset)**.** A *lattice* is a poset $\mathcal{L}$ satisfying that, for all $a, b \in \mathcal{L}$, both $\sup\{a, b\}$ and $\inf\{a, b\}$ exist in $\mathcal{L}$.

2.2. **Distributive Lattices.** An *n-ary operation on* $\mathcal{A}$ is a function $f : \mathcal{A}^n \to \mathcal{A}$ where n is the *arity* of f. A *finitary* operation f is an n-ary operation for some nonnegative integer $n \in \mathbb{N}$. f is nullary (or a constant) if its arity is zero, i.e. it is completely determined by the only element $\emptyset \in \mathcal{A}^0$, hence a nullary operation f on $\mathcal{A}$ can be identified with the element $f(\emptyset)$; for convenience it is regarded as an element of $\mathcal{A}$. An operation on $\mathcal{A}$ is *unary* or *binary* if its arity is 1 or 2, respectively.

Definition 2.3 (Universal algebra)**.** A *algebra* is an ordered pair $\mathbf{A} := (\mathcal{A}, \mathcal{F})$ where $\mathcal{A}$ is a nonempty set and $\mathcal{F}$ a family of finitary operations on $\mathcal{A}$. The set $\mathcal{A}$ is the *universe* or the *underlying set* of $\mathbf{A}$ and $\mathcal{F}$ the *fundamental operations* of $\mathbf{A}$.

An algebra is *finite* if the cardinality of its universe is bounded. When $\mathcal{F}$ is finite, say $\mathcal{F} = \{f_1, f_2, \cdots, f_k\}$, we also write $\mathbf{A} = (\mathcal{A}, f_1, f_2, \cdots, f_k)$ with the operations sorted by their arities in descending order. As a common example, a *group* is an algebra of the form $\mathbf{G} = (\mathcal{G}, \cdot, ^{-1}, 1)$ where $\cdot, ^{-1}, 1$ are a binary, a unary, and a nullary operations on $\mathcal{G}$, respectively.

Definition 2.4 (Lattice as an algebra)**.** A *lattice* is an algebra $\mathbf{L} := (\mathcal{L}, \mathcal{F})$ where $\mathcal{F}$ contains two binary operations $\vee$ and $\wedge$ (read "join" and "meet" respectively) on $\mathcal{L}$ that satisfy the following axiomatic identities for all $x, y, z \in \mathcal{L}$,

(LA-1) commutative laws: $x \vee y = y \vee x$, $x \wedge y = y \wedge x$;
(LA-2) associative laws: $x \vee (y \vee z) = (x \vee y) \vee z$, $x \wedge (y \wedge z) = (x \wedge y) \wedge z$;
(LA-3) absorption laws: $x = x \vee (x \wedge y)$, $x = x \wedge (x \vee y)$.

Sometimes the following idempotent laws are also included in the definition of a lattice although they can be derived from the above three axioms,

$$x \vee x = x, \qquad x \wedge x = x. \tag{2.1}$$

A lattice defined as a poset can be converted to an algebra by constructing the binary operations as $a \vee b = \sup\{a, b\}$ and $a \wedge b = \inf\{a, b\}$; the converse case can also be achieved by defining the partial order as $a \leq b \Leftrightarrow a = a \wedge b$. Hence Definition 2.2 and Definition 2.4 are equivalent.

Definition 2.5. A *bounded lattice* is an algebra $(\mathcal{L}, \mathcal{F})$ where $\mathcal{F}$ contains binary operations $\vee, \wedge$ and nullary operations $\hat{0}, \hat{1}$ so that $(\mathcal{L}, \vee, \wedge)$ is a lattice and, $\forall x \in \mathcal{L}$,

$$x \wedge \hat{0} = \hat{0}, \qquad x \vee \hat{1} = \hat{1}. \tag{2.2}$$

The boundedness in the above definition is best understood from the poset viewpoint: $\hat{0} \leq x$ and $x \leq \hat{1}$ for all $x \in \mathcal{L}$.

Definition 2.6. A *distributive lattice* is a lattice which satisfies either of the distributive laws

$$x \wedge (y \vee z) = (x \wedge y) \vee (x \wedge z), \qquad x \vee (y \wedge z) = (x \vee y) \wedge (x \vee z). \tag{2.3}$$

Either identity in (2.3) can be deduced from the other and DEFINITION 2.4 [5, p. 10].

A notion central to every branch of mathematics is isomorphism. In particular, two lattices are isomorphic if they have the same structure.

Definition 2.7 (Lattice isomorphism)**.** A *homomorphism* of the lattice $(\mathcal{L}_1, \vee, \wedge)$ into the lattice $(\mathcal{L}_2, \cup, \cap)$ is a map $\phi : \mathcal{L}_1 \to \mathcal{L}_2$ satisfying

$$\forall x, y \in \mathcal{L}_1, \quad \phi(x \vee y) = \phi(x) \cup \phi(y), \ \phi(x \wedge y) = \phi(x) \cap \phi(y). \tag{2.4}$$

An *isomorphism* is a bijective homomorphism.

More details on distributive lattices can be found in [5] from the perspective of universal algebra and in [37, ch. 3] from the viewpoint of posets. See [9] for a more accessible one.

2.3. **Boolean algebra.** The simplest definition may be due to Huntington [13].

Definition 2.8. A *Boolean algebra* is an algebra of the form

$$\mathbf{B} := (\mathcal{B}, \ \vee, \ \wedge, \ ', \ \hat{0}, \ \hat{1}), \tag{2.5}$$

where the binary operations $\vee$, $\wedge$, the unary operation $'$ called complementation, and the nullary operations $\hat{0}$, $\hat{1}$ satisfy

(BA-1) the identity laws: $x \wedge \hat{1} = x$, $x \vee \hat{0} = x$,
(BA-2) the complement laws: $x \wedge x' = \hat{0}$, $x \vee x' = \hat{1}$,
(BA-3) the commutative laws (LA-1),
(BA-4) the distributive laws (2.3).

Other definitions contain redundant axiomatic laws that can be deduced from the above four conditions. For example, Givant and Halmos [8, p. 10] defined a Boolean algebra as an algebra with its fundamental operations satisfying (LA-1), (LA-2), (2.1), (2.2), (2.3), (BA-1), (BA-2), $\hat{0}' = \hat{1}$, $\hat{1}' = \hat{0}$, $(x')' = x$, and the DeMorgan's laws,

$$(x \wedge y)' = x' \vee y', \qquad (x \vee y)' = x' \wedge y'. \tag{2.6}$$

In this work we adopt the viewpoint of Burris and Sankappanavar [5, p. 116].

Definition 2.9. A *Boolean algebra* is a bounded distributive lattice with an additional complementation operation that satisfies the complement laws (BA-2).

2.4. **Veblen's theorem.** A *graph* is an ordered pair $G = (V, E)$ where V is the set of *vertices* and E the set of *edges*, each edge being an *unordered* pair of distinct vertices. G' is a *subgraph* of G, written as $G' \subseteq G$, if $V(G') \subseteq V(G)$ and $E(G') \subseteq E(G)$. If $uv \in E(G)$, then u and v are *adjacent* in G, and the edge uv is said to be *incident* to u and v. The *degree* of a vertex v is the number of edges incident to v.

Definition 2.10. A *path* is a graph P of the form $V(P) = \{v_0, v_1, \ldots, v_\ell\}$ and $E(P) = \{v_0v_1, v_1v_2, \ldots, v_{\ell-1}v_\ell\}$. A *cycle* is a graph of the form $C := P + v_0v_\ell$ where P is a path and $\ell \geq 2$.

A graph G is *connected* if for every pair of distinct vertices in $V(G)$ there is a subgraph of G as the path from one vertex to the other. A *component* of the graph is a *maximal connected subgraph*.

Theorem 2.11 (Veblen [42])**.** *A graph can be partitioned into edge-disjoint cycles if and only if the degree of every vertex is even.*

Proof. If a graph is the union of a number of edge-disjoint cycles, then clearly a vertex contained in n cycles has degree $2n$. Hence the necessity holds.

Suppose that the degree of every vertex is a positive even integer. How do we find a single cycle in G? Let $P = x_0x_1\cdots x_\ell$ be a path of maximal length ℓ in G. Since $d(x_0) \geq 2$, x_0 must have another neighbor y in addition to x_1. Furthermore, we must have $y = x_i$ for some $i \in [2, \ell]$; otherwise it would contradict the starting condition that P is of maximal length. Therefore we have found a cycle $x_0x_1\cdots x_i$.

Having found one cycle, we remove it from G. If the remaining subgraph G_1 of G is not empty, then the degree of every vertex in G_1 remains positive and even. Repeating the cycle-finding procedures completes the proof; see [4, p. 5]. □

A *multigraph* is an augmented graph that allows *loop*s and *multiple edges*; the former is defined as a special edge joining a vertex to itself and the latter several edges joining the same vertices. A loop contributes 2 to the degree of a vertex while each edge in a multiple edge contribute 1. As for cycles, the condition of $\ell \geq 2$ in Definition 2.10 is changed to $\ell \geq 0$ for a multigraph: $\ell = 0$ indicates a loop and $\ell = 1$ two edges joining the same vertices. It is straightforward to extend Theorem 2.11 to multigraphs.

Theorem 2.12. *A multigraph can be partitioned into edge-disjoint cycles if and only if the degree of each vertex is positive and even.*

A *directed* graph/multigraph is a graph/multigraph where the edges are *ordered* pairs of vertices. An edge uv is then said to *start* at u and *end* at v. Furthermore, the degree of a vertex v is split into the *outdegree* $d^+(v)$ and the *indegree* $d^-(v)$, with the former as the number of edges starting at v and the latter that of edges ending at v. Veblen's Theorem generalizes to directed multigraphs in a straightforward manner.

Theorem 2.13. *A directed multigraph can be partitioned into directed cycles if and only if each vertex has the same outdegree and indegree.*

3. Yin sets

Based on regular semianalytic sets introduced in Section 3.1, we propose in Section 3.2 the Yin space for fluid modeling in two dimensions. From the viewpoint of Jordan curves in Section 3.3, we study in Section 3.4 the local and global topology of Yin sets, the results of which yield the notion of *realizable spadjors* in Section 3.5 as a unique boundary representation of Yin sets.

3.1. **Regular semianalytic sets.** In a topological space $\mathcal{X}$, the *complement* of a subset $\mathcal{P} \subseteq \mathcal{X}$, written $\mathcal{P}'$, is the set $\mathcal{X} \setminus \mathcal{P}$. The *closure* of a set $\mathcal{P} \subseteq \mathcal{X}$, written $\mathcal{P}^-$, is the intersection of all closed supersets of $\mathcal{P}$. The *interior* of $\mathcal{P}$, written $\mathcal{P}^\circ$, is the union of all open subsets of $\mathcal{P}$. The *exterior* of $\mathcal{P}$, written $\mathcal{P}^\perp := \mathcal{P}'^\circ := (\mathcal{P}')^\circ$, is the interior of its complement. By the identity $\mathcal{P}^- = \mathcal{P}'^{\circ\prime}$ [8, p. 58], we have $\mathcal{P}^\perp = \mathcal{P}^{-\prime}$. A point $\mathbf{x} \in \mathcal{X}$ is a *boundary point* of $\mathcal{P}$ if $\mathbf{x} \notin \mathcal{P}^\circ$ and $\mathbf{x} \notin \mathcal{P}^\perp$. The

boundary of $\mathcal{P}$, written $\partial\mathcal{P}$, is the set of all boundary points of $\mathcal{P}$. It can be shown that $\mathcal{P}^\circ = \mathcal{P} \setminus \partial\mathcal{P}$ and $\mathcal{P}^- = \mathcal{P} \cup \partial\mathcal{P}$. An open set $\mathcal{P} \subseteq \mathcal{X}$ is *regular* if it coincides with the interior of its own closure, i.e. if $\mathcal{P} = \mathcal{P}^{-\circ}$. A closed set $\mathcal{P} \subseteq \mathcal{X}$ is *regular* if it coincides with the closure of its own interior, i.e. if $\mathcal{P} = \mathcal{P}^{\circ-}$. The duality of the interior and closure operators implies $\mathcal{P}^\circ = \mathcal{P}'^{-\prime}$, hence $\mathcal{P}$ is a *regular open set* if and only if $\mathcal{P} = \mathcal{P}^{\perp\perp} := \left(\mathcal{P}^\perp\right)^\perp$. For any subset $Q \subseteq \mathcal{X}$, it can be shown that $Q^{\perp\perp}$ is a regular open set and $Q^{\circ-}$ is a regular closed set.

Regular sets, open or closed, capture the salient feature that physically meaningful regions are free of lower-dimensional elements such as isolated points and curves in 2D and dangling faces in 3D.

Theorem 3.1 (MacNeille [20] and Tarski [39])**.** *Let $\mathbb{B}$ denote the class of all regular open sets of a topological space $\mathcal{X}$ and define $\mathcal{P} \cup^{\perp\perp} \mathcal{Q} := (\mathcal{P} \cup \mathcal{Q})^{\perp\perp}$ for all $\mathcal{P}, \mathcal{Q} \subseteq \mathcal{X}$. Then $\mathbf{B}_o := (\mathbb{B},\ \cup^{\perp\perp},\ \cap,\ ^\perp,\ \emptyset,\ \mathcal{X})$ is a Boolean algebra.*

Proof. See [8, §10]. □

Similarly, it can be shown that, with appropriately defined operations, regular closed sets of a topological space $\mathcal{X}$ also form a Boolean algebra [17, p. 39].

Regular sets are not perfect for representing physically meaningful regions yet: some of them cannot be described by a finite number of symbol structures. For example, some sets have nowhere differentiable boundaries, which, in their parametric forms, are usually infinite series of continuous functions [33]. Another pathological case is more subtle: intersecting two regular sets with piecewise smooth boundaries may yield an infinite number of disjoint regular sets. Consider

$$\begin{cases} \mathcal{A}_p := \{(x,y) \in \mathbb{R}^2 : -2 < y < \sin\frac{1}{x},\ 0 < x < 1\}, \\ \mathcal{A}_s := \{(x,y) \in \mathbb{R}^2 : 0 < y < 1,\ -1 < x < 1\}. \end{cases} \tag{3.1}$$

Although both $\mathcal{A}_p$ and $\mathcal{A}_s$ are described by two inequalities, their intersection is a disjoint union of an infinite number of regular sets; see [28, Fig. 4-1, Fig. 4-2]. This poses a fundamental problem that results of Boolean operations of two regular sets may not be well represented on a computer by a finite number of entitites.

Therefore, we need to find a proper subspace of regular sets, each element of which is finitely describable. This search eventually arrives at semianalytic sets.

Definition 3.2. A set $\mathcal{S} \subseteq \mathbb{R}^{\mathsf{D}}$ is *semianalytic* if there exist a finite number of analytic functions $g_i : \mathbb{R}^{\mathsf{D}} \to \mathbb{R}$ such that $\mathcal{S}$ is in the universe of a finite Boolean algebra formed from the sets

$$\mathcal{X}_i = \left\{\mathbf{x} \in \mathbb{R}^{\mathsf{D}} : g_i(\mathbf{x}) \geq 0\right\}. \tag{3.2}$$

The g_i's are called the *generating functions* of $\mathcal{S}$. In particular, a semianalytic set is *semialgebraic* if all of its generating functions are polynomials.

Recall that a function is *analytic* if and only if its Taylor series at $\mathbf{x}_0$ converges to the function in some neighborhood for every $\mathbf{x}_0$ in its domain. In the example of (3.1), $\mathcal{A}_s$ is semianalytic while $\mathcal{A}_p$ is not, because the Taylor series of $g_2(x,y) := \sin\frac{1}{x} - y$ at the origin does not converge. Roughly speaking, the boundary curves of regular semianalytic sets are piecewise smooth.

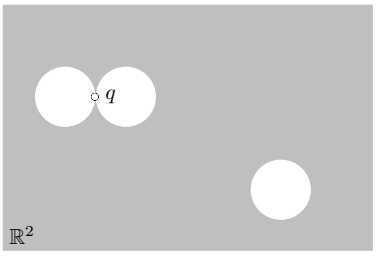

(a) an unbounded Yin set

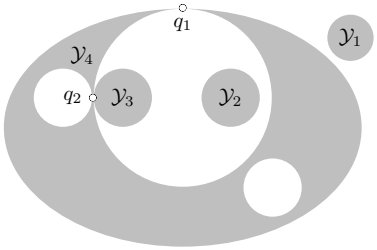

(b) a bounded Yin set

FIGURE 1. Examples of Yin sets. The Yin set in (a) is obtained by removing from $\mathbb{R}^2$ three closed balls, two of which share a common boundary point q. The Yin set in (b) is the union of four pairwise disjoint Yin sets $\mathcal{Y} = \bigcup_{i=1}^{4} \mathcal{Y}_i$, where $\mathcal{Y}_4$ is an open ellipse with three closed balls removed, two of which share a common boundary point q_2. The points q, q_1, q_2 are boundary points but not interior points of the Yet sets.

3.2. $\mathbb{Y}$**: the Yin space for fluid modeling.** Regular closed semianalytic sets have been an essential mathematical tool for solid modeling since the dawning time of this field [31]. However, as shown in Figure 5, requiring regular semianalytic sets to be closed would make their boundary representation not unique, degrading the isomorphism in Definition 3.20 and Theorem 3.21 to a homomorphism. As another work closely related to this one, the analysis on a family of interface tracking methods [43, 49] via the theory of donating regions [44, 45] also requires that the regular sets be open. Therefore, only regular open semianalytic sets are employed in this work.

Definition 3.3. A *Yin set*[1] $\mathcal{Y} \subseteq \mathbb{R}^2$ is a regular open semianalytic set whose boundary is bounded. The class of all such Yin sets form the *Yin space* $\mathbb{Y}$.

In Figure 1, the Yin set in subplot (a) is unbounded and connected while that in subplot (b) is bounded and consists of four disjoint components.

By Definition 3.2, semianalytic sets are closed under set complementation, finite union, and finite intersection. Then by Theorem 3.1, regular open semianalytic sets form a Boolean algebra since they are the intersection of the universes of two Boolean algebras. Furthermore, Boolean operations on Yin sets preserve the attribute of a bounded boundary being bounded, hence we have

Theorem 3.4. *The algebra* $\mathbf{Y} := (\mathbb{Y},\ \cup^{\perp\perp},\ \cap,\ ^{\perp},\ \emptyset,\ \mathbb{R}^2)$ *is a Boolean algebra.*

3.3. **Jordan curves and orientations.** A *path* in $\mathbb{R}^2$ from p to q is a continuous map $f : [0, 1] \to \mathbb{R}^2$ satisfying $f(0) = p$ and $f(1) = q$. A subset $\mathcal{P}$ of $\mathbb{R}^2$ is *path-connected* if every pair of points of $\mathcal{P}$ can be joined by a path in $\mathcal{P}$. Given $\mathcal{Q} \subset \mathbb{R}^2$, define an equivalence relation on $\mathcal{Q}$ by setting $x \sim y$ if there is a path-connected

[1]Yin sets are named after the first author's mentor, Madam Ping Yin. As a coincidence, the most important dichotomy in Taoism consists of Yin and Yang, where Yang represents the active, the straight, the ascending, and so on, while Yin represents the passive, the circular, the descending, and so on. From this viewpoint, straight lines and Jordan curves can be considered as Yang 1-manifolds and Yin 1-manifolds, respectively.

subset of Q that contains both x and y. The equivalence classes are called the *path-connected component*s of $\mathcal{Q}$.

A *planar curve* is a continuous map $\gamma : (0,1) \to \mathbb{R}^2$. It is *piecewise analytic* if the map is the composite of a finite number of analytic functions. It is *simple* if the map is injective; otherwise it is *self-intersecting*. Although strictly speaking a curve γ is a map, we also use γ to refer to its image. Two distinct curves γ_1 and γ_2 *intersect* at q if there exist $s_1, s_2 \in (0,1)$ such that $\gamma_1(s_1) = \gamma_2(s_2) = q$. Then q is the *intersection* of γ_1 and γ_2. For an open ball $\mathcal{N}_r(q)$ with sufficiently small radius r, $\mathcal{N}_r(q) \setminus \gamma_1$ consists of two disjoint connected regular open sets. If $\gamma_2 \setminus q$ is entirely contained in one of these two sets, q is an *improper intersection*; otherwise it is a *proper intersection*. Two curves are *disjoint* if they have neither proper intersections nor improper ones. Suppose upon its extension to a path, a simple curve γ further satisfies $\gamma(0) = \gamma(1)$, then γ is a *simple closed curve* or *Jordan curve*.

Theorem 3.5 (Jordan Curve Theorem [14])**.** *The complement of a Jordan curve γ in the plane $\mathbb{R}^2$ consists of two components, each of which has γ as its boundary. One component is bounded and the other is unbounded; both of them are open and path-connected.*

The above theorem states that a Jordan curve divides the plane into three parts: itself, its *interior*, and *exterior*.

Definition 3.6. The *interior* of an oriented Jordan curve γ, denoted by $\mathrm{int}(\gamma)$, is the component of the complement of γ that always lies to the left when an observer traverses the curve in the increasing direction of the parameterization s.

A Jordan curve is said to be *positively oriented* if its interior is the bounded component of its complement; otherwise it is *negatively oriented*. The orientation of a Jordan curve can be flipped by reversing the increasing direction of the parameterization. The following notion will be used throughout this work.

Definition 3.7. Two Jordan curves are *almost disjoint* if they have no proper intersections and at most a finite number of improper intersections.

3.4. **The local and global topology of a Yin set.** The following lemma characterizes the local topology of a Yin set at its boundary.

Lemma 3.8. *Let $p \in \partial\mathcal{Y}$ be a boundary point of a Yin set $\mathcal{Y} \subset \mathbb{R}^2$ and denote by $\mathcal{N}_r(p)$ the open ball centered at p with its radius $r > 0$. For any sufficiently small r,*

(a) $\partial\mathcal{Y} \cap \mathcal{N}_r(p)$ consists of $n_c(p)$ simple curves, where $n_c(p)$ is a finite positive integer,
(b) if $n_c(p) > 1$, all simple curves in (a) intersect and p is their sole intersection,
(c) $\mathcal{N}_r(p) \setminus \partial\mathcal{Y}$ consists of an even number of disjoint regular open sets; for two such sets sharing a common boundary, one is a subset of $\mathcal{Y}$ while the other that of $\mathcal{Y}^\perp$.

Proof. Since $\mathcal{Y}$ is semianalytic, Definition 3.2 implies that $\mathcal{Y} \cap \mathcal{N}_r(p)$ is defined by a finite number of analytic functions $g_i : \mathbb{R}^2 \to \mathbb{R}$. By the implicit function theorem, each $g_i(\mathbf{x}) = 0$ defines a planar curve. Then (a) and (b) follows from the condition of $\mathcal{Y}$ being regular open and the condition that $r > 0$ can be as small as one wishes.

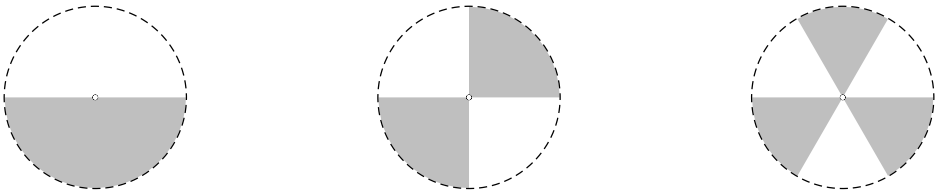

(a) one curve (b) two curves (c) three or more

FIGURE 2. The local topology at a boundary point p (open dot) of a Yin set $\mathcal{Y}$ (shaded region). The dashed circle represents the boundary of $\mathcal{N}_r(p)$, a local neighborhood of p. The open dot in subplot (c) corresponds to the boundary point q_2 in Figure 1(b) while that in subplot (b) to q, q_1 in Figure 1(a), (b). All other boundary points in Figure 1 correspond to that in subplot (a).

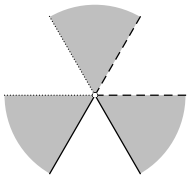

FIGURE 3. Decomposing the boundary $\partial\mathcal{Y}$ of a connected Yin set $\mathcal{Y}$ into a set of Jordan curves by disentangling the multiple boundary curves that intersect at a boundary point q (the hollow dot). This example corresponds to Figure 2 (b) and (c). The shaded fan-shaped wedges represent connected components of $\mathcal{Y} \cap \mathcal{N}_r(q)$, and the white fan-shaped wedges those of $\mathcal{Y}^\perp \cap \mathcal{N}_r(q)$. Two simple curves incident to q are assigned to the same Jordan curve if they are part of the boundary of the same component of $\mathcal{Y}^\perp \cap \mathcal{N}_r(p)$.

Hence the local topology at a boundary point p can be characterized by the number of the aforementioned curves that intersect at p, as is shown in Figure 2.

By (a), (b), and the fact of $\mathcal{N}_r(p)$ being regular open, $\mathcal{N}_r(p) \setminus \partial\mathcal{Y}$ consists of an even number of disjoint regular open sets. Consider two such sets that share a common boundary. Suppose both of them are subsets of $\mathcal{Y}$, then it contradicts the fact of $\mathcal{Y}$ being regular. Suppose both of them are subsets of $\mathcal{Y}^\perp$, then it contradicts the fact of their common boundary being a subset of $\partial\mathcal{Y}$. Hence (c) follows. □

The above lemma on the local topology naturally yields a result on the global topology of a connected Yin set.

Theorem 3.9. *For a connected Yin set $\mathcal{Y} \neq \emptyset, \mathbb{R}^2$, its boundary $\partial\mathcal{Y}$ can be uniquely partitioned into a finite set of pairwise almost disjoint Jordan curves.*

Proof. Without loss of generality, we focus on a single connected component of $\partial\mathcal{Y}$. By Lemma 3.8, a boundary point $q \in \partial\mathcal{Y}$ can be classified into two types according to n_c, the number of curves that intersect at q.

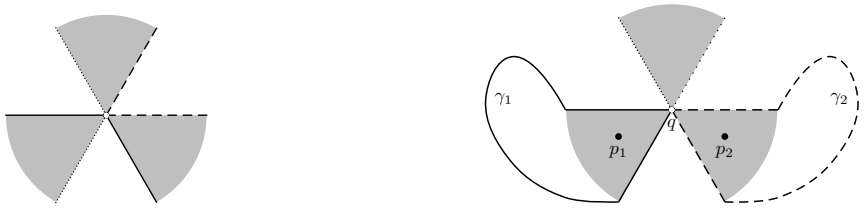

(a) The boundary Jordan curves have proper intersections

(b) $\mathcal{Y}$ becomes disconnected

FIGURE 4. The decomposition method shown in Figure 3 is the only valid choice to decompose the boundary of a *connected* Yin set into pairwise almost disjoint Jordan curves, because any other choice yields a contradiction.

If all boundary points satisfy $n_c = 1$, the condition of $\partial\mathcal{Y}$ being bounded implies that this connected component of $\partial\mathcal{Y}$ must be a single Jordan curve. Hence the statement holds trivially.

Otherwise a finite number of boundary points satisfy $n_c > 1$. Then we construct a multigraph $G_{\partial\mathcal{Y}}$ by setting its vertex set as $\{q\}$ and by obtaining its edges from dividing $\partial\mathcal{Y}$ with $\{q\}$. By Lemma 3.8 (a), (b), and $\partial\mathcal{Y}$ being connected, the degree of each vertex in $G_{\partial\mathcal{Y}}$ is even. Then it follows from Theorem 2.12 that we can decompose $\partial\mathcal{Y}$ into edge-disjoint cycles. As shown in Figure 3, the decomposition is performed by requiring that, at each vertex q, two edges incident to q are assigned to the same cycle if and only if they belong to the boundary of the same connected component of $\mathcal{Y}^\perp \cap \mathcal{N}_r(q)$. Consequently, no edges in different cycles intersect properly at each self-intersection, hence the resulting Jordan curves are pairwise almost disjoint.

Finally, we show that the decomposition in Figure 3 is the only valide choice. Consider the other possibilities shown in Figure 4. If the two edges in the same cycle are not adjacent as in Figure 4 (a), then two cycles would have a proper intersection at q, which contradicts the condition of the Jordan curves having no proper intersections. As for the last possibility shown in Figure 4 (b), two edges in the same cycle are adjacent but they both belong to the boundary of some connected component of $\mathcal{Y} \cap \mathcal{N}_r(p)$. Then we can draw Jordan curves $\gamma_1, \gamma_2 \subset \partial\mathcal{Y}$ that contain them. The simpleness of a Jordan curve implies $\gamma_1 \neq \gamma_2$. Then there exist two points $p_1, p_2 \in \mathcal{Y}$ that belong to the bounded complements of γ_1 and γ_2, respectively. Because $\mathcal{Y}$ is connected, there exists a path within $\mathcal{Y}$ that connects p_1 and p_2. By Theorem 3.5, this path has to intersect γ_1 at some point, say p_c. The construction of this path implies $p_c \in \mathcal{Y}$; the construction of γ_1 implies $p_c \in \partial\mathcal{Y}$. This is a contradiction because $\mathcal{Y}$ is open. □

The above proof hinges on the fact of a Yin set being open, so Theorem 3.9 may not hold for the closure of a Yin set. As shown in Figure 5, the decomposition of the boundary of a regular closed set is *not* unique. This is a main reason that we do not model physically meaningful regions with regular closed sets.

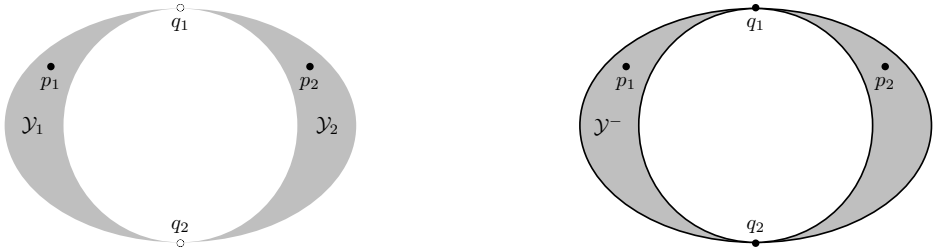

(a) $\mathcal{Y} = \mathcal{Y}_1 \cup \mathcal{Y}_2$; $\mathcal{Y}_1 \cap \mathcal{Y}_2 = \emptyset$; $q_1, q_2 \notin \mathcal{Y}$ (b) $\mathcal{Y}^- = \mathcal{Y}_1^- \cup \mathcal{Y}_2^-$; $q_1, q_2 \in \mathcal{Y}^-$

FIGURE 5. Theorem 3.9 does not hold for the closure of a Yin set. In (a), the Yin set $\mathcal{Y}$ consists of two disjoint components $\mathcal{Y}_1$ and $\mathcal{Y}_2$ that share two common boundary points q_1 and q_2. In (b), the closure of $\mathcal{Y}$, $\mathcal{Y}^- = \mathcal{Y} \cup \partial\mathcal{Y}$, becomes connected. The solid curves indicate that $\mathcal{Y}^-$ is a regular closed set. The crucial difference is that, after the closure of $\mathcal{Y}$, the two points p_1, p_2 that previously belong to the two disjoint Yin sets in (a) can now be joined by a path in $\mathcal{Y}^-$. Consequently, the decomposition of $\partial\mathcal{Y}^-$ into a set of pairwise almost disjoint Jordan curves is not unique any more.

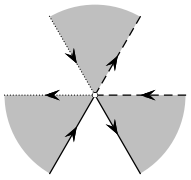

FIGURE 6. Decomposing connected $\partial\mathcal{Y}$ into a set of oriented Jordan curves. The connected Yin set $\mathcal{Y}$ is represented by shaded regions. The Jordan curves determined by the choice shown in Figure 3 can be uniquely oriented by requiring that $\mathcal{Y}$ always lies at the left of each curve.

To relate $\mathcal{Y}$ to its boundary Jordan curves, we first define a partial order on Jordan curves.

Definition 3.10 (Inclusion of Jordan curves)**.** A Jordan curve γ_k is said to *include* γ_ℓ, written as $\gamma_k \geq \gamma_\ell$ or $\gamma_\ell \leq \gamma_k$, if and only if the bounded complement of γ_ℓ is a subset of that of γ_k. If γ_k includes γ_ℓ and $\gamma_k \neq \gamma_\ell$, we write $\gamma_k > \gamma_\ell$ or $\gamma_\ell < \gamma_k$.

Definitions 2.1 and 3.10 yield a covering relation for Jordan curves.

Definition 3.11 (Covering of Jordan curves)**.** Let $\mathcal{J}$ denote a poset of Jordan curves with inclusion as the partial order. We say γ_k *covers* γ_ℓ in $\mathcal{J}$ and write '$\gamma_k \succ \gamma_\ell$' or '$\gamma_\ell \prec \gamma_k$' if $\gamma_\ell < \gamma_k$ and no elements $\gamma \in \mathcal{J}$ satisfies $\gamma_\ell < \gamma < \gamma_k$.

Now we state the most important result of this subsection.

Theorem 3.12. *Suppose a Yin set $\mathcal{Y} \neq \emptyset, \mathbb{R}^2$ is connected. Then the Jordan curves as the unique decomposition of $\partial\mathcal{Y}$, given by the method shown in Figure 3,*

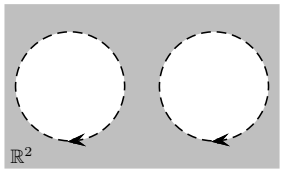

(a) two incomparable negatively oriented Jordan curves

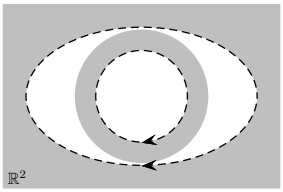

(b) two comparable negatively oriented Jordan curves

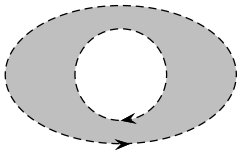

(c) a positively oriented Jordan curve covers a negatively oriented one

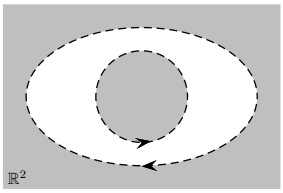

(d) a negatively oriented Jordan curve covers a positively oriented one

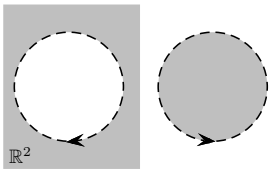

(e) two incomparable Jordan curves with different orientations

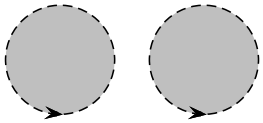

(f) two incomparable positively oriented Jordan curves

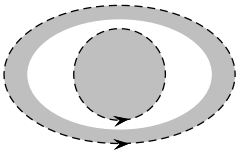

(g) two comparable positively oriented Jordan curves

FIGURE 7. Enumerating all cases of two oriented almost disjoint Jordan curves γ_1 and γ_2 with respect to their orientations and inclusion relations. This is useful in proving Theorem 3.12: if γ_1 and γ_2 are in the unique decomposition of the boundary of a connected Yin set $\mathcal{Y}$ and we require that $\mathcal{Y}$ always be at the left side of both γ_1 and γ_2, then only (a) and (c) are valid, because (b), (e), and (g) contradict the fact of both γ_1 and γ_2 are part of the boundary of $\mathcal{Y}$ and (d) and (f) contradict the condition of $\mathcal{Y}$ being connected.

can further be uniquely oriented such that

$$\mathcal{Y} = \bigcap_{\gamma_j \in \mathcal{J}_{\partial\mathcal{Y}}} \operatorname{int}(\gamma_j). \tag{3.3}$$

$\mathcal{J}_{\partial\mathcal{Y}}$, the set of oriented boundary Jordan curves of $\mathcal{Y}$, must be one of the two types,

$$\begin{cases} \mathcal{J}^- = \{\gamma_1^-, \gamma_2^-, \ldots, \gamma_{n_-}^-\}, & n_- \geq 1, \\ \mathcal{J}^+ = \{\gamma^+, \gamma_1^-, \gamma_2^-, \ldots, \gamma_{n_-}^-\}, & n_- \geq 0, \end{cases} \tag{3.4}$$

where all γ_j^-'s are negatively oriented, mutally incomparable with respect to inclusion. For $\mathcal{J}^+$, we also have

$$\forall j = 1, 2, \ldots, n_-, \quad \gamma_j^- \prec \gamma^+. \tag{3.5}$$

Proof. As in the proof of Theorem 3.9, we construct a multigraph $G_{\partial\mathcal{Y}}$ from $\partial\mathcal{Y}$. $G_{\partial\mathcal{Y}}$ is further made a directed multigraph via orienting $\partial\mathcal{Y}$ so that $\mathcal{Y}$ always lies at the left side of any oriented Jordan curve. As shown in Figure 6, the indegree and outdegree of any vertex in $G_{\partial\mathcal{Y}}$ equals. By Theorem 2.13, there exists at least one directed cycle decomposition of $\partial\mathcal{Y}$. Then the uniqueness of the directed cycle decomposition follows from the uniqueness of orienting the Jordan curves in Figure 6.

Consider the case $\mathcal{J}_{\partial\mathcal{Y}} = \mathcal{J}^-$. For $n_- > 1$, suppose that γ_1^- and γ_2^- is comparable, as shown in Figure 7(b). According to the orientation, $\mathcal{Y}$ must lie at the left side of both γ_1^- and γ_2^-, but this is impossible because both γ_1^- and γ_2^- are part of the boundary of $\mathcal{Y}$. Consequently, (3.3) follows from Definition 3.6; see Figure 7(a).

Consider the case $\mathcal{J}_{\partial\mathcal{Y}} = \mathcal{J}^+$. If $n_- = 0$, then (3.5) holds vacuously and (3.3) holds trivially from Definition 3.6. For $n_- > 0$, suppose (3.5) did not hold for a negatively oriented Jordan curve γ_1^-. Then the almost disjointness implies that either $\gamma^+ \prec \gamma_1^-$ or they are not comparable. Suppose the former case holds, a path from one point at the left of γ^+ to another point at the left of γ_1^- must contain some points not in $\mathcal{Y}$, which contradicts the condition of $\mathcal{Y}$ being connected; see Figure 7 (d). The latter case does not hold either because it contradicts the fact that γ^+ is part of the boundary of $\mathcal{Y}$; see Figure 7 (e). Hence (3.5) must hold. By arguments in the previous paragraph, the negatively oriented Jordan curves must also be pairwise incomparable. Therefore, (3.3) follows from Definition 3.6; see Figure 7 (c).

Suppose $\mathcal{J}_{\partial\mathcal{Y}}$ contains two positively oriented Jordan curves γ_1, γ_2. Then their almost disjointness implies that $\mathrm{int}(\gamma_1)$ is either in the unbounded complement or the bounded complement of γ_2. By similar arguments, the former contradicts the fact of $\mathcal{Y}$ being connected, as in Figure 7 (f), and the latter contradicts the fact of both γ_1 and γ_2 are part of the boundary of $\mathcal{Y}$, as in Figure 7 (f). Hence $\mathcal{J}_{\partial\mathcal{Y}}$ contains at most one positively oriented Jordan curve. This completes the proof. □

Corollary 3.13. *Each Yin set $\mathcal{Y} \neq \emptyset, \mathbb{R}^2$ can be uniquely expressed as*

$$\mathcal{Y} = \bigcup\nolimits_j^{\perp\perp} \bigcap_i \mathrm{int}\left(\gamma_{j,i}\right), \tag{3.6}$$

where j is the index of connected components of $\mathcal{Y}$ and $\gamma_{j,i}$'s are oriented Jordan curves that are pairwise almost disjoint.

Proof. The conclusion follows from applying Theorem 3.12 to each connected component of $\mathcal{Y}$. □

We illustrate (3.3) and (3.6) by the two distinct types of Yin sets in Figure 8.

By results on the global topology, it is straightforward to identify the Betti numbers of a Yin set with the numbers of oriented Jordan curves in its representation.

Corollary 3.14. *The number of holes in a connected Yin set is the number of negatively oriented Jordan curves in the unique expression (3.3). The number of connected components in a bounded Yin set is the number of positively oriented Jordan curves in the unique expression (3.6).*

This simple result is due to the topological stratification of the Yin space and the natural correspondence of holes to negatively oriented Jordan curves.

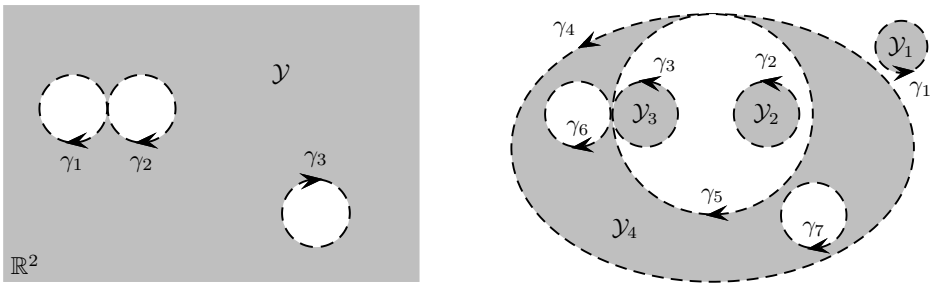

(a) a connected Yin set (b) a Yin set with four connected components

FIGURE 8. Orienting boundary Jordan curves of the Yin sets in Figure 1 as illustrations of the two types of connected Yin sets classified in Theorem 3.12. In subplot (a), $\mathcal{Y} = \bigcap_{j=1}^{3} \operatorname{int}(\gamma_j)$; in subplot (b), $\mathcal{Y} = \bigcup_{i=1}^{4} \mathcal{Y}_i = \operatorname{int}(\gamma_1) \cup \operatorname{int}(\gamma_2) \cup \operatorname{int}(\gamma_3) \cup \left[\bigcap_{j=4}^{7} \operatorname{int}(\gamma_j)\right]$. By Theorem 3.12, the boundaries of the connected Yin sets $\mathcal{Y}$ in (a) and $\mathcal{Y}_4$ in (b) are of the types $\mathcal{J}^-$ and $\mathcal{J}^+$, respectively.

3.5. $\mathbb{J}$**: representing Yin sets via realizable spadjors.** Our starting point is the following acronym.

Definition 3.15. A *spadjor* is a nonempty set $\mathcal{J}_k$ of pairwise almost disjoint, piecewise-analytic oriented Jordan curves.

The following boundary-to-interior map ρ assigns to each spadjor a Yin set,

$$\rho(\mathcal{J}_k) := \bigcap\nolimits_{\gamma_i \in \mathcal{J}_k} \operatorname{int}(\gamma_i). \tag{3.7}$$

Not all spadjors are useful for representing Yin sets. The global topology of Yin sets in Theorem 3.12 and Corollary 3.13 naturally suggests that we should limit our attention to certain types of spadjors.

Definition 3.16. An *atom spadjor* is a spadjor $\mathcal{J}_k$ that consists of at most one positively oriented Jordan curve γ^+ and a finite number of negatively oriented Jordan curves γ_1^-, γ_2^-, …, $\gamma_{n_-}^-$ such that

(a) γ_j^-'s are pairwise incomparable with respect to inclusion,
(b) $\gamma_\ell^- \prec \gamma^+$ for each $\ell = 1, 2, \ldots, n_-$,
(c) $\rho(\mathcal{J}_k)$ is a connected Yin set.

Since a spadjor cannot be an empty set, $n_- = 0$ implies the presence of γ^+ and the absence of γ^+ implies $n_- > 0$. By definition, an atom spadjor is in the form of either $\mathcal{J}^-$ or $\mathcal{J}^+$ in (3.4).

Definition 3.17. A *realizable spadjor* $\mathcal{J} = \cup_k \mathcal{J}_k$ is the union of a finite number of atom spadjors such that $\mathcal{J}_i$ and $\mathcal{J}_j$ being distinct implies $\rho(\mathcal{J}_i) \cap \rho(\mathcal{J}_j) = \emptyset$.

Intuitively, an atom spadjor represents a connected Yin set while a realizable spadjor may represent a Yin set with multiple connected components. For example, the Yin set in Figure 8(b) can be represented by the realizable spadjor

$$\mathcal{J} = \left\{\gamma_1^+, \gamma_4^+, \gamma_6^-, \gamma_5^-, \gamma_7^-, \gamma_2^+, \gamma_3^+\right\}. \tag{3.8}$$

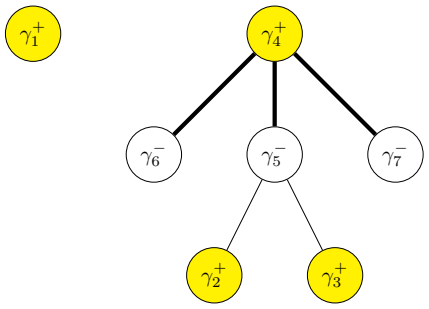

FIGURE 9. The Hasse diagram for the realizable spadjor $\mathcal{J}$ in (3.8) that represents the Yin set in Figure 8(b). The partial order is the "inclusion" relation as in Definition 3.10. A shaded circle represents a positively oriented Jordan curve while an unshaded circle a negatively oriented Jordan curve. The partition of $\mathcal{J}$ into atom spadjors consists of two steps: (a) form an atom spadjor from each shaded circle and its immediate children (if there is any) and (b) if any unshaded circles remain, group them into $\mathcal{J}^-$. These two steps correspond to (R2A-a,b) in Lemma 3.18.

Lemma 3.18 concerns recovering the atom spadjors in a realizable spadjor.

Lemma 3.18. *Any realizable spajor $\mathcal{J}$ can be* uniquely *expressed as*

$$\mathcal{J} = \cup_{i=1}^{n} \mathcal{J}_i^+ \cup \mathcal{J}^-, \tag{3.9}$$

where the $\mathcal{J}_i^+$'s and the $\mathcal{J}^-$ are extracted from $\mathcal{J}$ as follows.

(R2A-a) For each positively oriented Jordan curve $\gamma_i^+ \in \mathcal{J}$, form an atom spadjor $\mathcal{J}^+$ by adding γ_i^+ and all negatively oriented Jordan curves covered by γ_i^+.

(R2A-b) If there are negatively oriented Jordan curves left in $\mathcal{J}$, group them into an atom spadjor $\mathcal{J}^-$.

Proof. The existence of the expression in (3.9) follows from Definition 3.17 and Theorem 3.12. As for the uniqueness, we first note that at most one atom spadjor in the form of $\mathcal{J}^-$ can be extracted from any realizable spadjor; otherwise it would contradict the condition $\rho(\mathcal{J}_i) \cap \rho(\mathcal{J}_j) = \emptyset$ in Definition 3.17. Second, $\mathcal{J}^- \neq \emptyset$ and $n > 0$ imply that the positively oriented Jordan curve γ_k^+ of any $\mathcal{J}_k^+ \subset \mathcal{J}$ is covered by a negatively oriented element $\gamma_i^- \in \mathcal{J}^-$. Third, any negatively oriented Jordan curve not belonging to $\mathcal{J}^-$ can be *covered* by at most one $\mathcal{J}_k^+$. □

The partition of a realizable spadjor $\mathcal{J}$ into atom spadjors is best illustrated by the Hasse diagram of the poset $\mathcal{J}$ with respect to inclusion, c.f. Figure 9.

Definition 3.19. The *Jordan space* is the set

$$\mathbb{J} := \{\hat{0}, \hat{1}\} \cup \{\mathcal{J}\} \tag{3.10}$$

where $\{\mathcal{J}\}$ denotes the set of all realizable spadjors and $\hat{0}$, $\hat{1}$ are two symbols satisfying

$$\rho(\hat{0}) := \emptyset, \qquad \rho(\hat{1}) := \mathbb{R}^2. \tag{3.11}$$

One can interpret $\hat{0}$ and $\hat{1}$ as atom spadjors consisting of a single oriented Jordan curve with infinitesimal diameter such that its interior goes to $\emptyset$ and $\mathbb{R}^2$, respectively.

It now makes sense to extend the definition of the boundary-to-interior map in (3.7) and (3.11) to the Jordan space.

Definition 3.20. The *boundary-to-interior map* $\rho : \mathbb{J} \to \mathbb{Y}$ associates a Yin set with each element in the Jordan space as

$$\rho(\mathcal{J}) := \begin{cases} \emptyset & \text{if } \mathcal{J} = \hat{0}; \\ \mathbb{R}^2 & \text{if } \mathcal{J} = \hat{1}; \\ \bigcup^{\perp\perp}_{\mathcal{J}_j \subset \mathcal{J}} \bigcap_{\gamma_i \in \mathcal{J}_j} \mathrm{int}(\gamma_i) & \text{otherwise,} \end{cases} \tag{3.12}$$

where the $\mathcal{J}_i$'s are atom spadjors extracted from $\mathcal{J}$ as in Lemma 3.18.

Theorem 3.21. *The boundary-to-interior map in Definition 3.20 is bijective.*

Proof. For the Yin sets $\emptyset$ and $\mathbb{R}^2$, (3.11) states that $\hat{0}$ and $\hat{1}$ are their preimages. For any other Yin set $\mathcal{Y} \neq \emptyset, \mathbb{R}^2$, we can uniquely decompose it as $\mathcal{Y} = \bigcup^{\perp\perp}_{\mathcal{Y}_i \subseteq \mathcal{Y}} \mathcal{Y}_i$, where the connected components $\mathcal{Y}_i$'s are pairwise disjoint. By Theorem 3.12, each $\mathcal{Y}_i$ is uniquely expressed as the intersection of interiors of a number of oriented Jordan curves. Hence ρ is surjective. Also, ρ is injective because of the uniqueness in Lemma 3.18. □

Corollary 3.22. *A Yin set is uniquely represented by a realizable spadjor.*

Proof. This follows from Theorem 3.21 and Corollary 3.13. □

We sum up this section by Figure 10, where a physically meaningful region with complex topology is modeled by a fun Yin set, which is further uniquely represented by a realizable spadjor.

4. The Boolean algebra on Yin sets

After introducing the pasting map in Section 4.1, we define in Sections 4.2 and 4.3 the complementation and the meet operations on realizable spadjors to equip the Jordan space $\mathbb{J}$ as a bounded distributive lattice. Along the way, we show that these operations are counterparts to Boolean operations on the Yin space. Our theory culminates in Section 4.4. In Section 5.3, we discuss implementation issues and present a fun example of our Boolean algorithms on Yin sets.

4.1. The pasting map of realizable spadjors.

The following cutting map is trivial, but its inverse in Lemma 4.2 is not. They are crucial for the complementation and the meet operations in Sections 4.2 and 4.3.

Definition 4.1. For a realizable spadjor $\mathcal{J}$, let V denote a finite point set that contains all intersections of the Jordan curves in $\mathcal{J}$. The associated *cutting map* or *segmentation map* S_V assigns to $\mathcal{J}$ a set E of oriented paths obtained by dividing the oriented Jordan curve in $\mathcal{J}$ at points in V. The set of (oriented) paths $E = S_V(\mathcal{J})$ is called a *segmented realizable spadjor*.

Lemma 4.2. *The realizable spadjor $\mathcal{J} = S_V^{-1}(E)$ corresponding to a segmented realizable spadjor E can be uniquely constructed as follows.*

(S2R-a) Remove all self-loops in E and insert them into $\mathcal{J}$.

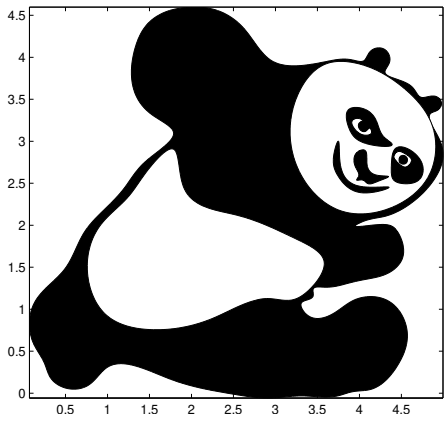

(a) a panda modeled as a Yin set $\mathcal{P}$

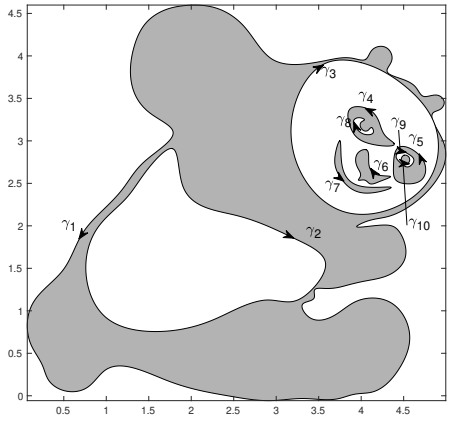

(b) the unique representation of $\mathcal{P}$ as a realizable spadjor $\mathcal{J}$

FIGURE 10. A Yin set with complex topology and geometry. In subplot (b), the Jordan curves γ_1, γ_4, γ_5, γ_6, γ_7, and γ_{10} are positively oriented while the others are negatively oriented. The realizable spadjor is $\mathcal{J} = \cup_{k=1}^{6}\mathcal{J}_k$, with the atom spadjors as $\mathcal{J}_1 = \{\gamma_1, \gamma_2, \gamma_3\}$, $\mathcal{J}_2 = \{\gamma_4, \gamma_8\}$, $\mathcal{J}_3 = \{\gamma_5, \gamma_9\}$, $\mathcal{J}_4 = \{\gamma_6\}$, $\mathcal{J}_5 = \{\gamma_7\}$, and $\mathcal{J}_6 = \{\gamma_{10}\}$; all atom spadjors are of the type $\mathcal{J}^+$ in (3.4). The panda is uniquely expressed as $\mathcal{P} = \cup_{k=1}^{6}\mathcal{P}_k = \rho(\mathcal{J})$ with each connected component as $\mathcal{P}_k = \rho(\mathcal{J}_k)$. The picture in subplot (a) is a raster image while the curves in subplot (b) are cubic splines fit through a total of 120 points. This small amount of points demonstrates the efficiency of realizable spadjor in representing complex topology and geometry.

(S2R-b) Start with a path $\beta_{in} \in E$ and denote by $v \in V$ its ending point. If there exists only one path whose starting point is v, call it β_{out} and append it to β_{in}. Otherwise, set β_{out} to be the edge that starts at v and of which the positive counter-clockwise angle $\angle\beta_{out}v\beta_{in}$ is the smallest. Repeat the above conditional to grow the path until it becomes a loop γ_1, and remove from E all paths that constitute γ_1.

(S2R-c) If γ_1 is a Jordan curve, add it into $\mathcal{J}$; otherwise divide γ_1 into Jordan curves and/or self-loops and add them into $\mathcal{J}$.

(S2R-d) Repeat (S2R-b,c) to add other Jordan curves into $\mathcal{J}$ until E becomes empty.

Proof. First we note that Theorem 3.9 is not applicable here because the Yin set $\rho(\mathcal{J})$ may be disconnected. By Definition 3.6, the Yin set $\rho(\mathcal{J})$ always lies at the left of any oriented path $\beta \in E$, the steps (S2R-a,b) are sufficient to fulfill this invariant. The choice for growing the path in (S2R-b) also avoids potential proper intersections of Jordan curves in $\mathcal{J}$; see Figure 4(a). However, as suggested by Figure 4(b) and the proof of Theorem 3.9, the loop γ_1 might not be a single Jordan curve, hence we need to divide it into Jordan curves and/or self-loops in (S2R-c);

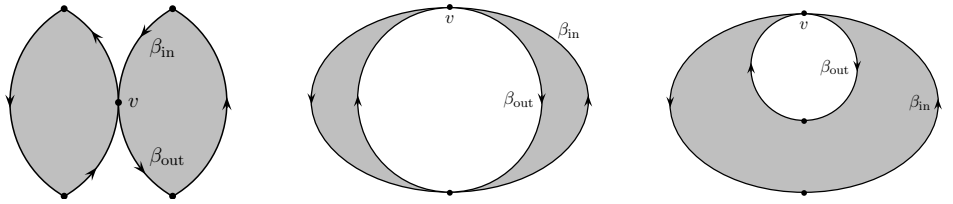

(a) Two components and one improper intersection

(b) Two components and two improper intersections

(c) One component and one improper intersection

FIGURE 11. Illustrating key steps (S2R-b,c) of the pasting map in Lemma 4.2. The shaded region represents a Yin set, whose boundary consists of two Jordan curves with an improper intersection at v. In each subplot, the solid dots represent points of V while the directed paths constitute E. Starting from β_{in}, we pick β_{out} to grow the starting path because $\angle\beta_{\text{out}}v\beta_{\text{in}}$ is the smallest counterclockwise angle among those of the two out-edges; this condition in (S2R-b) is different from that in Figure 3. In subplot (c), the loop γ_1 resulting from (S2R-b) consumes all paths. Hence in (S2R-c) we divide it into two Jordan loops to fulfill the representation invariant of realizable spadjors.

see Figure 11. The uniqueness of the constructed realizable spadjor follows from the uniqueness in Corollary 3.22. □

The procedures in Lemma 4.2 define the inverse of the cutting map, to which we refer as the *pasting map of realizable spadjors*.

4.2. **Complementation: a unitary operation on $\mathbb{J}$.** The following is an easy result on the local topology of regular sets.

Corollary 4.3. *Suppose $\mathcal{Y}$ is a regular open or regular closed set. Then a point $p \in \mathbb{R}^2$ is a boundary point of $\mathcal{Y}$ if and only if, for any sufficiently small $r > 0$, the open ball $\mathcal{N}_r(p)$ centered at p with radius r contains both points in $\mathcal{Y}$ and $\mathcal{Y}^\perp$.*

Proof. The necessity follows directly from Lemma 3.8 (c), we only prove the sufficiency. If r is sufficiently small, there are only seven cases for the type of points contained in $\mathcal{N}_r(p)$: (i) $\mathcal{Y}$, (ii) $\mathcal{Y}^\perp$, (iii) $\partial\mathcal{Y}$, (iv) $\mathcal{Y}$ and $\mathcal{Y}^\perp$, (v) $\mathcal{Y}$ and $\partial\mathcal{Y}$, (vi) $\mathcal{Y}^\perp$ and $\partial\mathcal{Y}$, and (vii) all three sets. Because of the regularity, cases (iii) to (vi) are impossible. By definitions in Section 3.1, (i) implies an interior point and (ii) implies an exterior point. Hence (vii) must imply a boundary point. In other words, the presence of $\mathcal{Y}$ and $\mathcal{Y}^\perp$ in $\mathcal{N}_r(p)$ dictates that of $\partial\mathcal{Y}$ in $\mathcal{N}_r(p)$. □

Corollary 4.3 and Lemma 4.2 motivate our complementation operation on $\mathbb{J}$.

Definition 4.4. The *complementation operation* $' : \mathbb{J} \to \mathbb{J}$ is defined as

$$\mathcal{J}' := \begin{cases} \hat{1} & \text{if } \mathcal{J} = \hat{0}; \\ \hat{0} & \text{if } \mathcal{J} = \hat{1}; \\ \left(S_V^{-1} \circ R \circ S_V\right) \mathcal{J} & \text{otherwise,} \end{cases} \tag{4.1}$$

where V is the set of improper intersections of Jordan curves in $\mathcal{J}$ and the orientation-reversing map R reverses the orientation of each path in the segmented realizable spadjor $S_V(\mathcal{J})$.

Lemma 4.5. *The complementation operation in Definition 4.4 satisfies*

$$\forall \mathcal{J} \in \mathbb{J}, \qquad \rho(\mathcal{J}') = (\rho(\mathcal{J}))^{\perp}. \tag{4.2}$$

Proof. By definition, a regular set $\mathcal{Y}$ satisfies $(\mathcal{Y}^{\perp})^{\perp} = \mathcal{Y}$, which, together with Corollary 4.3, imply that $\mathcal{Y}$ and $\mathcal{Y}^{\perp}$ have exactly the same boundary. By Corollary 3.13 and Definition 3.6, the realizable spadjors representing $\mathcal{Y}$ and $\mathcal{Y}^{\perp}$ are the same set of Jordan curves except that each pair of corresponding Jordan curves has different orientations, which justifies the necessity of the orientation-reversing map R. More precisely, the conjugate of R by the cutting map S_V is needed here because one or multiple improper intersections of two Jordan curves may dictate that the paths constituting oriented Jordan curves in $\mathcal{J}$ be reorganized in order to represent $\mathcal{Y}^{\perp}$ properly. For example, the calculation of $\mathcal{Y}^{\perp}$ for the Yin set $\mathcal{Y}$ in Figure 11 (b) involves not only reversing the orientation of each path, but also reorganizing these paths into different Jordan curves. □

4.3. **Meet: a binary operation on $\mathbb{J}$.** To define the meet of two realizable spadjors $\mathcal{J}$ and $\mathcal{K}$, we cut them by S_V, select those paths that are on the boundary of the Yin set $\rho(\mathcal{J}) \cap \rho(\mathcal{K})$, and paste the set of selected paths by S_V^{-1} to form the result. Lemma 4.6 and Corollary 4.7 tell us which paths we should choose.

Lemma 4.6. *Denote $\mathcal{Y} := \mathrm{int}(\sigma_1) \cap \mathrm{int}(\sigma_2)$ where σ_1 and σ_2 are two oriented Jordan curves. For a curve β satisfying $\beta \subseteq \sigma_1$ and $\beta \subset \mathbb{R}^2 \setminus \sigma_2$, we have $\beta \subseteq \partial\mathcal{Y}$ if and only if $\beta \subset \mathrm{int}(\sigma_2)$. For a curve β satisfying $\beta \subseteq \sigma_1 \cap \sigma_2$, we have $\beta \subseteq \partial\mathcal{Y}$ if and only if the direction of β induced from the orientation of σ_1 is the same as that induced from the orientation of σ_2.*

Proof. We only prove the first statement since the second one can be shown similarly. By Definition 3.6, $\mathrm{int}(\sigma_1)$ and $\mathrm{int}(\sigma_2)$ are both Yin sets. It follows from Theorem 3.4 that $\mathcal{Y}$ is also a Yin set. By Corollary 4.3, it suffices to show that a small open ball $\mathcal{N}_r(p)$ centered at $p \in \beta$ contains both points in $\mathcal{Y}$ and $\mathcal{Y}^{\perp}$ if and only if $\beta \subset \mathrm{int}(\sigma_2)$. As shown in Figure 12, $p \in \beta$ and $\beta \subseteq \sigma_1$ imply that $\mathcal{N}_r(p) \cap \mathrm{int}(\sigma_1) \neq \emptyset$; then the condition $\beta \subset \mathrm{int}(\sigma_2)$ implies $\mathcal{N}_r(p) \cap \mathcal{Y} \neq \emptyset$. DeMorgan's law (2.6) yields

$$\mathcal{Y}^{\perp} = [\mathrm{int}(\sigma_1) \cap \mathrm{int}(\sigma_2)]^{\perp} = \mathrm{int}(\sigma_1)^{\perp} \cup^{\perp\perp} \mathrm{int}(\sigma_2)^{\perp} \neq \emptyset,$$

which, together with $\beta \subseteq \sigma_1$, imply $\mathcal{N}_r(p) \cap \mathcal{Y}^{\perp} \neq \emptyset$. By Corollary 4.3, we have $\beta \subset \partial\mathcal{Y}$. Conversely, $\beta \not\subset \mathrm{int}(\sigma_2)$, $\beta \subset \mathbb{R}^2 \setminus \sigma_2$, and $\beta \subseteq \sigma_1$ imply that $\mathcal{N}_r(q) \cap \mathcal{Y} = \emptyset$ for all $q \in \beta$. These arguments are illustrated in Figure 12. □

Hereafter we write the union of all Jordan curves in a realizable spadjor as

$$P(\mathcal{J}) := \bigcup_{\gamma_i \in \mathcal{J}} \gamma_i, \tag{4.3}$$

which is clearly a subset of $\mathbb{R}^2$.

Corollary 4.7. *Denote $\mathcal{Y} := \rho(\mathcal{J}) \cap \rho(\mathcal{K})$ where $\mathcal{J}$ and $\mathcal{K}$ are two realizable spadjors. For a curve β satisfying $\beta \subseteq P(\mathcal{J})$ and $\beta \subset \mathbb{R}^2 \setminus P(\mathcal{K})$, we have $\beta \subseteq \partial\mathcal{Y}$ if and only if $\beta \subset \rho(\mathcal{K})$. For a curve β satisfying $\beta \subseteq P(\mathcal{J}) \cap P(\mathcal{K})$, we have $\beta \subseteq \partial\mathcal{Y}$*

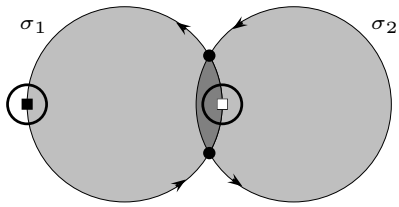

FIGURE 12. In proving Lemma 4.6, we consider $\mathcal{Y} := \mathrm{int}(\sigma_1) \cap \mathrm{int}(\sigma_2)$ where σ_1 and σ_2 are two oriented Jordan curves. By Corollary 4.3, $\beta \subset \partial\mathcal{Y}$ if and only if for any point $p \in \beta$ (the open square), any sufficiently small neighborhood of p contains both points in $\mathcal{Y}$ and $\mathcal{Y}^\perp$. On the other hand, if a point q (the filled square) is not in σ_2, then it is definitely not on the boundary of $\mathcal{Y}$.

if and only if the direction of β induced from the orientation of $\mathcal{J}$ is the same as that induced from the orientation of $\mathcal{K}$.

Proof. This follows directly from Lemma 4.6. □

Definition 4.8. The *meet of two realizable spadjors* $\mathcal{J}$ and $\mathcal{K}$ is a binary operation $\wedge : \mathbb{J} \times \mathbb{J} \to \mathbb{J}$ defined as

$$\mathcal{J} \wedge \mathcal{K} = \begin{cases} \hat{0} & \text{if } \mathcal{K} = \hat{0}; \\ \mathcal{J} & \text{if } \mathcal{K} = \hat{1}; \\ S_V^{-1}(E) & \text{otherwise,} \end{cases} \tag{4.4}$$

where the pasting map S_V^{-1} is defined in Lemma 4.2, and the directed multigraph (V, E) is constructed as follows.

(MRS-a) The set $\mathcal{I} := P(\mathcal{J}) \cap P(\mathcal{K})$ may contain paths and isolated points. Initialize V as an empty set; add into V all path endpoints and isolated points in $\mathcal{I}$.

(MRS-b) Cut $\mathcal{J}$ with points in V and we have a set of paths $\{\beta_i\} = S_V(\mathcal{J})$. Initialize E as an empty set.

(MRS-c) For each β_i, add it to E if β_i minus its endpoints is contained in $\rho(\mathcal{K})$, or, if there exists $\beta_j \subset P(\mathcal{K})$ such that $\beta_j = \beta_i$ and they have the same direction. In particular, if β_i is a Jordan curve that satisfies either of the above conditions, we insert β_i as a self-loop into E.

(MRS-d) For each $\beta_j \subset S_V(\mathcal{K})$, add it to E if β_j minus its endpoints is contained in $\rho(\mathcal{J})$.

Lemma 4.9. *The meet operation in Definition 4.8 satisfies*

$$\forall \mathcal{J}, \mathcal{K} \in \mathbb{J}, \qquad \rho(\mathcal{J} \wedge \mathcal{K}) = \rho(\mathcal{J}) \cap \rho(\mathcal{K}). \tag{4.5}$$

Proof. Denote $\mathcal{Y}_\cap := \rho(\mathcal{J}) \cap \rho(\mathcal{K})$. It follows from Corollary 4.7 that each path $\beta_i \subset S_V(\mathcal{J})$ is added to E in step (MRS-c) if and only if $\beta_i \subset \partial\mathcal{Y}_\cap$; similarly, each curve $\beta_j \subset S_V(\mathcal{K})$ is added to E in step (MRS-d) if and only if $\beta_j \subset \partial\mathcal{Y}_\cap$. Hence the union of the vertices and edges in G constitute the boundary of $\mathcal{Y}_\cap$. Furthermore, by the difference between (MRS-c) and (MRS-d), each edge on $\partial\mathcal{Y}_\cap$ is inserted into E only once. Therefore, E contains and only contains points on $\partial\mathcal{Y}_\cap$. The proof is then completed by Lemma 4.2 and Corollary 3.22. □

4.4. **The Yin space $\mathbb{Y}$ and the Jordan space $\mathbb{J}$ are isomorphic.** The join operation can be expressed by the meet operation and the complementation operation; this is also true for all other Boolean operations.

Definition 4.10. The *join of two realizable spadjors* $\mathcal{J}$ and $\mathcal{K}$ is a binary operation $\vee : \mathbb{J} \times \mathbb{J} \to \mathbb{J}$ defined as

$$\forall \mathcal{J}, \mathcal{K} \in \mathbb{J}, \qquad \mathcal{J} \vee \mathcal{K} := (\mathcal{J}' \wedge \mathcal{K}')'. \tag{4.6}$$

The following theorem is the theoretical culmination of this paper.

Theorem 4.11. *The Boolean algebras* $(\mathbb{J}, \vee, \wedge, ', \hat{0}, \hat{1})$ *and* $(\mathbb{Y}, \cup^{\perp\perp}, \cap, ^{\perp}, \emptyset, \mathbb{R}^2)$ *are isomorphic under the boundary-to-interior map* ρ *in Definition 3.20.*

Proof. This follows directly from Lemmas 4.5 and 4.9, Definitions 3.20 and 4.10, and DeMorgan's law (2.6). □

As the desired consequence, we have reduced the two-dimensional problems $\cup^{\perp\perp}$, $\cap$, and $^{\perp}$ to the one-dimensional problems $\vee$, $\wedge$, and $'$.

5. Boolean algorithms on Yin sets

Purely algebraic and constructive as they are, Definitions 4.4, 4.8, and 4.10 already constitute a complete set of Boolean algorithms on Yin sets. In this section we discuss important details on algorithmic design and implementations, state main results on the analysis of algorithmic complexity, and perform a variety of test cases to validate our theory and to verify our implementation. In particular, the utilities of our Boolean algorithms in tracking deforming fluid phases are demonstrated by results of a standard benchmark test.

We do not expect the reader to be able to implement our Boolean algorithms after reading this section. Instead, the exposition in this section is only intended to give the reader a relatively complete picture on *theoretical* aspects of Boolean algorithms on the Yin space. We will fully explain the algorithmic details of our implementation in another separate paper.

5.1. **User-friendly design.** The input is an indispensable part of an algorithm, and a user-friendly design of input parameters adds to the appealingness of an algorithm.

In our implementation, the data structure that represents Yin sets is designed to be a straightforward orchestration of the realizable spadjor, i.e., a set of point arrays where each array represents a polygon and the direction of points in the array indicates the orientation of the polygon. To input Yin sets, the user does not need to specify the inclusion relations of the boundary Jordan curves: we have encapsulated the computation of this information inside the algorithms. So long as each input is indeed a realizable spadjor, the algorithm returns the correct result. In the meantime, the user can choose to output the results in the same format of the input; she can also output the Hasse diagram of the results with respect to the inclusion relation. These designs make the software interface simple, flexible, and user-friendly.

5.2. **Robustness.** Our algorithm is distinguished from other Boolean algorithms in that the user is given an explicit control on the uncertainty of Boolean operations.

Given a small positive real number ϵ, we define two points to be the same point if their distance is smaller than ϵ. A consistent enforcement of this definition and its implications across the entire package makes our implementation robust and provides an effective mechanism to handle various degenerate cases that characterize topological changes.

It is well known in the community of computational geometry that intersecting line segments might lead to unavoidable self-inconsistencies and cause a program to abort at the run time [16]. The mathematical core of this difficulty is the potentially arbitrary ill-conditioning of intersecting line segments in an unlimited range of length scales. Fortunately, in the context of numerically simulating multiphase flows, there always exists a length scale h below which finer details are not needed. Hence this uncertain parameter ϵ is not only a device of flexibility and convenience, but more importantly a simple solution of the aforementioned robustness problem in computational geometry.

5.3. **Implementation.** Implementing Boolean operations in Section 4 reduce to two well-studied problems in computational geometry: one is to determine the relative positions of a set of points to a simple polygon, and the other is to compute intersections of the edges of two simple polygons.

We solve these two problems based on the line sweep idea in [2][7, Chap. 2], but our solutions differ from current methods in several aspects. First, we enforce the uncertainty criterion in Section 5.2 to deal with overlapping of line segments for robust floating-point calculations. Second, we modify traditional algorithms to cater for our problems. For example, the point-in-polygon algorithm in [24, Sec. 7.4] designed for determine the relative position of a *single* point to a polygon with n edges has complexity $O(n)$. Repeatedly applying this algorithm to q points would have the overall complexity $O(qn)$; this is not optimal if the number of points is large. Based on the idea of line sweep, we developed another algorithm with complexity $O((n+q)\log n)$.

We have implemented these algorithms and tested them thoroughly by a series of test cases; some fun examples are shown in Figure 13.

5.4. **Complexity.** In discussing complexity, we restrict realizable spadjors to be constituted by *linear* polygons only.

Let n denote the total number of points in two realizable spadjors that represent two Yin sets. Let I denote the number of their intersections. It can be shown that the complexity of our implementation of the meet operation in Definition 4.8 is $O((n+I)\log n)$. As for the complementation operation, the complexity is $O(n)$ where now n denotes the number of points in the single spadjor.

Our algorithm of constructing the Hasse diagram for a realizable spadjor has the worst-case complexity $O(m(m+l)\log l)$, where m is the number of polygons in the spadjor and l is the maximum number of points of these polygons.

5.5. **Applications to interface tracking.** As discussed in Section 1.2, a deforming fluid phase is usually represented by a point set $\mathcal{M}(t) := \{\mathbf{x} : f(\mathbf{x},t) = 1\}$ where f is the color function as defined in (1.2). Then the interface tracking (IT) problem can be regarded as the determination of $\mathcal{M}(T)$ from the initial condition $\mathcal{M}(t_0)$ and the given velocity field $\mathbf{u}(\mathbf{x},t)$, $t \in [t_0, T]$. This approach is adopted

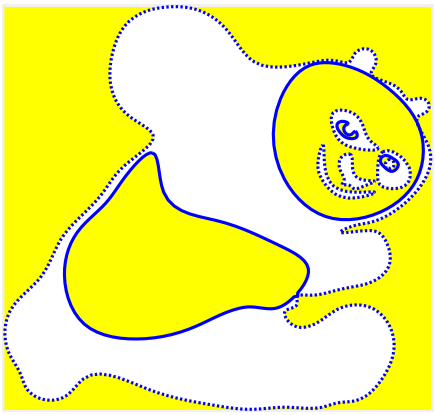

(a) $\mathcal{P}^{\perp}$: the exterior of the panda $\mathcal{P}$ in Figure 10 obtained by the complementation operation in Definition 4.4.

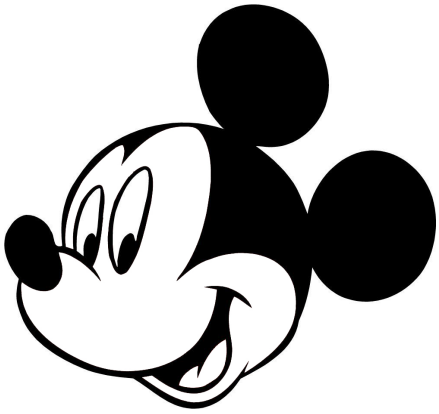

(b) a Mickey mouse modeled as a Yin set $\mathcal{M}$

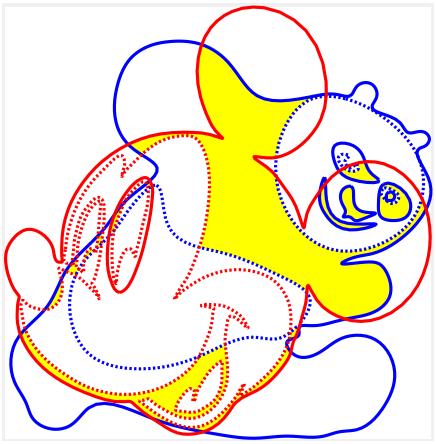

(c) $\mathcal{M} \cap \mathcal{P}$: intersection of $\mathcal{M}$ and $\mathcal{P}$ obtained by the meet operation in Definition 4.8.

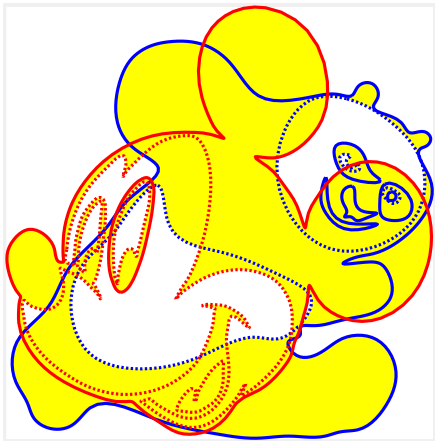

(d) $\mathcal{M} \cup^{\perp\perp} \mathcal{P}$: regularized union of $\mathcal{M}$ and $\mathcal{P}$ obtained by the join operation in Definition 4.10.

FIGURE 13. Results of testing Boolean algorithms on Yin sets with complex topology and geometry. In subplots (a), (c), and (d), a solid line represents a positively oriented Jordan curve, a dotted line a negatively oriented Jordan curve, and a shaded region the result of a Boolean operation. There are several improper intersections of the Jordan curves in the realizable spadjor that represents the panda.

for the error analysis of IT methods under the Lebesgue measure [49]. However, to deal with topological issues, it is necessary to refine the modeling of fluid phases via Yin sets so that the IT problem can be defined more precisely.

Definition 5.1 (the IT problem)**.** The *interface tracking problem* is the determination of the final loci of the fluid phase $\mathcal{M}(T) \in \mathbb{Y}$ by passively advecting $\mathcal{M}(t_0) \in \mathbb{Y}$,

TABLE 1. Geometric errors and convergence rates of the vortex-shear test [48, §5.2]. The parameters of the cubic MARS method are set to $h_L = 0.2h$ and $r_{\text{tiny}} = 0.01$. For any given h, we set the initial condition to a Yin set with piecewise linear boundaries that approximates the panda, compute volume fractions of the panda inside the control volumes, run the vortex-shear test to the ending time, calculate the difference of the two sets of volume fractions at the initial time and the ending time, and sum up the difference to obtain the geometric error. Over all time steps, the zeroth Betti number of the yellow region is 6, the first Betti number of the largest connected component is 2, those of components homeomorphic to the two eyes is 1, and those of all other connected components are 0.

$h = \frac{1}{32}$	rate	$h = \frac{1}{64}$	rate	$h = \frac{1}{128}$	rate	$h = \frac{1}{256}$
2.11e-03	2.61	3.46e-04	2.70	5.33e-05	2.88	7.23e-06

the initial loci of the phase, with a velocity field $\mathbf{u} : \mathbb{R}^{\mathsf{D}} \times [t_0, T] \to \mathbb{R}^{\mathsf{D}}$, where $\mathbf{u}$ is continuous in time $t \in [t_0, T]$ and piecewise Lipschitz continuous in space.

From this viewpoint, fluid phases deform according to the action of the flow map of the velocity field upon the Yin space. Here we only require piecewise Lipschitz continuity on the velocity field so that fluid modeling via Yin sets admits topological changes such as merging. On the other hand, when the flow map is a homeomorphism, all topological information should be preserved by the flow map.

We have coupled the recent cubic MARS method [48] to the Boolean algorithms on Yin sets; the result is a more versatile method capable of handling complex topology on very coarse grids. Given $\mathcal{M}^n \approx \mathcal{M}(t_n)$, major steps of our IT method are as follows.

(IT-1) Apply the flow map to vertices of linear polygons that represent $\mathcal{M}^n \in \mathbb{Y}$ to obtain their images;
(IT-2) Add or delete points between two adjacent markers if the distance of their images is too large or too small, respectively, so that all distances of adjacent marker images are within the interval $[r_{\text{tiny}} h_L, h_L]$;
(IT-3) Connect the marker images to obtain a Yin set $\mathcal{M}^{n+1}$ as the *global* solution;
(IT-4) Calculate the Betti numbers of $\mathcal{M}^{n+1}$ if needed;
(IT-5) Intersect $\mathcal{M}^{n+1}$ to fixed control volumes of length h to obtain *local* solutions.

In Step (IT-4), the Betti numbers of the tracked fluid phase are calculated in $O(1)$ time. To the best of our knowledge, no IT methods are even capable to calculate these Betti numbers. We also emphasize that the local solutions are important in coupling IT with high-order numerical solvers of the fluid phase. The reader is referred to [48] for other details.

In Table 1 and Figure 14, we show results of the standard vortex-shear test to demonstrate (1) the linear representation of the panda yields second-order convergence rates IT, and (2) the complex topology is preserved very well by the homeomorphic flow map, i.e. the Betti numbers of the fluid phase remain constants during the whole simulation. The details of this coupled method will be reported in another paper.

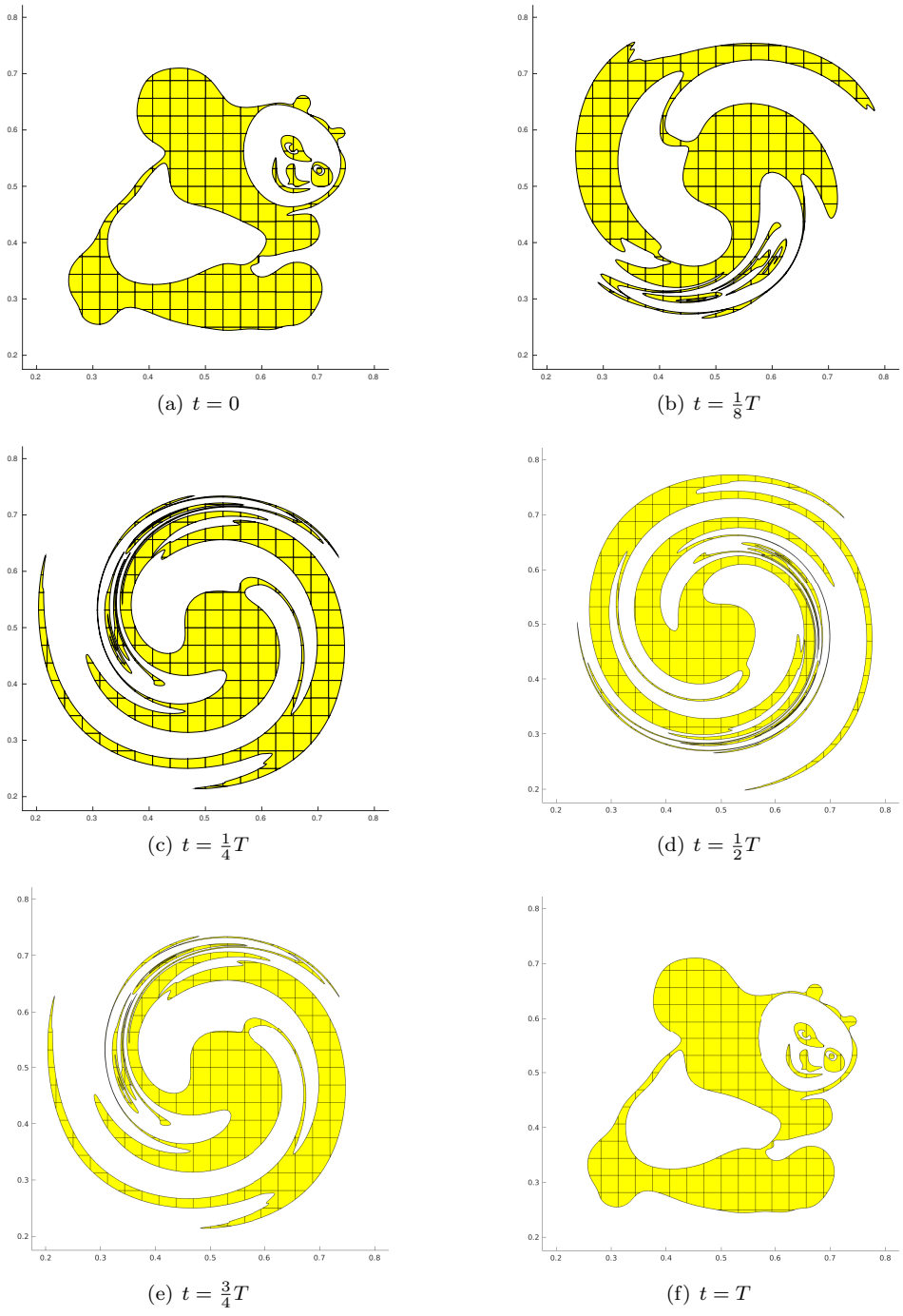

(a) $t = 0$ (b) $t = \frac{1}{8}T$

(c) $t = \frac{1}{4}T$ (d) $t = \frac{1}{2}T$

(e) $t = \frac{3}{4}T$ (f) $t = T$

FIGURE 14. Results of the cubic MARS method for the vortex shear test [48, §5.2] with $T = 8$, $h = \frac{1}{32}$, $h_L = 0.2h$, $r_{\mathsf{tiny}} = 0.01$, and the panda in Figure 10 (a) as the initial condition. Over all time steps, the number of connected components remain a constant and the number of holes in each connected component also remains a constant. These Betti numbers are returned in constant time.

6. Conclusion

We have introduced the problem of fluid modeling in multiphase flows as a counterpart of solid modeling in CAD, and have proposed to solve this problem via the Yin space, a topological space with a simple, efficient, and complete Boolean algebra. Under this framework, topological changes of Yin sets can be characterized and handled naturally and topological information such as Betti numbers can be extracted in constant time.

Several prospects for future research follow. The theory and algorithms on the Yin space can be generalized to 2-manifolds in a straightforward manner. Another generalization of Yin sets to three dimensions is currently a work in progress. Finally, it would be exciting to couple Yin sets with high-order finite-volume methods [46] to form fourth- and higher-order solvers for simulating multiphase flows such as free-surface flows and fluid-structure interactions.

Acknowledgments. The authors thank Difei Hu for digitizing the panda image, and Sen Li for generating the results of the vortex-shear test.

References

[1] Y. Bazilevs, K. Takizawa, and T. E. Tezduyar, *Computational fluid-structure interaction: Methods and applications*, Wiley Series in Computational Mechanics, Wiley, 2013.

[2] J. L. Bentley and T. A. Ottmann, *Algorithms for reporting and counting geometric intersections*, IEEE Trans. Comput. **C-28** (1979), 643–647.

[3] H. Bieri, *Nef polyhedra: A brief introduction*, Geometric Modelling (Vienna) (H. Hagen, G. Farin, and H. Noltemeier, eds.), Springer Vienna, 1995, pp. 43–60.

[4] B. Bollobás, *Modern graph theory*, corrected ed., Graduate Texts in Mathematics, vol. 184, Springer-Verlag, New York, 2008, ISBN:0-387-98488-7.

[5] S. Burris and H. P. Sankappanavar, *A course in universal algebra*, the millennium ed., Springer, 2012, ISBN:978-0-9880552-0-9.

[6] J. A. Cottrell, T. J. R. Hughes, and Y. Bazilevs, *Isogeometric analysis: Toward integration of CAD and FEA*, Wiley, Chichester, 2009.

[7] M. de Berg, O. Cheong, M. van Kreveld, and M. Overmars, *Computational geometry: Algorithms and applications*, 3rd ed., Springer, 2008.

[8] S. Givant and P. Halmos, *Introduction to Boolean algebras*, Springer, 2009.

[9] G. Grätzer, *Lattice theory: First concepts and distributive lattices*, Dover, 2009.

[10] G. Greiner and K. Hormann, *Efficient clipping of arbitrary polygons*, ACM Transactions on Graphics **17** (1998), no. 2, 71–83.

[11] P. Hachenberger, L. Kettner, and K. Mehlhorn, *Boolean operations on 3D selective Nef complexes: Data structure, algorithms, optimized implementation and experiments*, Computational Geometry: Theory and Applications **38** (2007), 64–99.

[12] C. W. Hirt and B. D. Nichols, *Volume of fluid (VOF) method for the dynamics of free boundaries*, J. Comput. Phys. **39** (1981), 201–225.

[13] E. V. Huntington, *Sets of independent postulates for the algebra of logic*, Trans. Amer. Math. Soc. **5** (1904), no. 3, 288–309.

[14] C. Jordan, *Cours D'Aanlyse l'École Polytechnique*, Paris, 1887, pp 587-594.

[15] T. Kaczynski, K. Mischaikow, and M. Mrozek, *Computational homology*, Applied Mathematical Sciences, vol. 157, Springer, 2004, ISBN: 978-0387408538.

[16] L. Kettner, K. Mehlhorn, S. Pion, S. Schirra, and C. Yap, *Classroom examples of robustness problems in geometric computations*, Computational Geometry: Theory and Applications **40** (2008), 61–78, doi:10.1016/j.comgeo.2007.06.003.

[17] K. Kuratowski and A. Mostowski, *Set theory, with an introduction to descriptive set theory*, Studies in Logic and the Foundations of Mathematics, vol. 86, North-Holland Publishing Co., Amsterdam, 1976, ISBN: 978-0720404708.

[18] Y.-D. Liang and B. A. Barsky, *An analysis and algorithm for polygon clipping*, Communications of the ACM **26** (1983), 868–877.

[19] Y. K. Liu, X. Q. Wang, S. Z. Bao, M. Gombosi, and B. Zalik, *An algorithm for polygon clipping, and for determining polygon intersections and unions*, Computers & Geosciences **33** (2007), 589–598.
[20] H. MacNeille, *Partially ordered sets*, Trans. Amer. Math. Soc. **42** (1937), 416–460.
[21] F. Martinez, C. Ogayar, J. R. Jimenez, and A. J. Rueda, *A simple algorithm for Boolean operations on poygons*, Advances in Engineering Software **64** (2013), 11–19.
[22] J. R. Munkres, *Elements of algebraic topology*, Perseus Publishing, Cambridge, Massachusetts, 1984, ISBN:0-201-04586-9.
[23] W. Nef, *Beiträge zur theorie der polyeder*, Herbert Lang, Bern, 1978.
[24] J. O'Rourke, *Computational geometry in c*, second ed., Cambridge University Press, New York, NY, USA, 1998.
[25] S. Osher and J. A. Sethian, *Fronts propagating with curvature-dependent speed: Algorithms based on Hamilton-Jacobi formulations*, J. Comput. Phys. **79** (1988), 12–49.
[26] Y. Peng, J.-H. Yong, W.-M. Dong, H. Zhang, and J.-G. Sun, *A new algorithm for Boolean operations on general polygons*, Computers & Graphics **29** (2005), 57–70.
[27] J. Qian and C. K. Law, *Regimes of coalescence and separation in droplet collision*, J. Fluid Mech. **331** (1997), 59–80.
[28] A. A. G. Requicha, *Mathematical models of rigid solid objects*, Technical Memorandum 28, The University of Rochester, Rochester NY, November 1977.
[29] A. A. G. Requicha and H. B. Voelcker, *Solid modeling: current status and research directions*, IEEE Computer Graphics and Applications **3** (1983), no. 7, 25–37.
[30] A. G. Requicha, *Representations for rigid solids: Theory, methods, and systems*, ACM Computing Surveys **12** (1980), 437–464, http://doi.acm.org/10.1145/356827.356833.
[31] A. G. Requicha and R. B. Tilove, *Mathematical foundations of constructive solid geometry: General topology of closed regular sets*, Tech. report, University of Rochester, Rochester, N.Y., 1978, `http://hdl.handle.net/1802/1209`.
[32] M. Rivero and F. R. Feito, *Boolean operations on general planar polygons*, Computers & graphics **24** (2000), 881–896.
[33] H. Sagan, *An elementary proof that Schoenberg's space-filling curve is nowhere differentiable*, Mathematics Magazine **65** (1992), no. 2, 125–128.
[34] P. Saveliev, *Topology illustrated*, Peter Saveliev, 2016, ISBN: 978-1495188756.
[35] V. Shapiro, *Solid modeling*, Handbook of Computer Aided Geometric Design (G. Farin, J. Hoschek, and M.-S. Kim, eds.), Elsevier Science Publishers, 2002, pp. 473–518.
[36] L. J. Simonson, *Industrial strength polygon clipping: A novel algorithm with applications in VLSI CAD*, Computer-Aided Design **42** (2010), no. 12, 1189–1196.
[37] R. P. Stanley, *Enumerative combinatorics: Volume 1*, 2nd ed., Cambridge Studies in Advanced Mathematics, vol. 49, Cambridge University Press, 2012, ISBN:978-1107602625.
[38] E. E. Sutherland and G. W. Hodgeman, *Rentrant polygon clipping*, Communications of the ACM **17** (1974), no. 1, 32–42.
[39] A. Tarski, *über additive and multiplikative Mengenkörper und Mengenfunktionen*, Sprawozdania z Posiedzeń Towarzystwa Naukowego Warszawskiego, Wydzial III Nauk Matematyczno-fizycznych **30** (1937), 151–181.
[40] G. Tryggvason, B. Bunner, D. Juric, W. Tauber, S. Nas, J. Han, N. Al-Rawahi., and Y.-J. Jan, *A front-tracking method for the computations of multiphase flow*, J. Comput. Phys. **169** (2001), 708–759.
[41] B. R. Vatti, *A generic solution to polygon clipping*, Communications of the ACM **35** (1992), no. 7, 56–63.
[42] O. Veblen, *An application of modular equations in analysis situs*, Annals of Mathematics, Second Series **14** (1912-1913), no. 1/4, 86–94, `http://www.jstor.org/stable/1967604`.
[43] Q. Zhang, *On a family of unsplit advection algorithms for volume-of-fluid methods*, SIAM J. Numer. Anal. **51** (2013), no. 5, 2822–2850.
[44] ———, *On donating regions: Lagrangian flux through a fixed curve*, SIAM Review **55** (2013), no. 3, 443–461.
[45] ———, *On generalized donating regions: Classifying Lagrangian fluxing particles through a fixed curve in the plane*, J. Math. Anal. Appl. **424** (2015), no. 2, 861–877.
[46] ———, *GePUP: Generic projection and unconstrained PPE for fourth-order solutions of the incompressible Navier-Stokes equations with no-slip boundary conditions*, J. Sci. Comput. **67** (2016), 1134–1180.

[47] ———, *HFES: a height function method with explicit input and signed output for high-order estimations of curvature and unit vectors of planar curves*, SIAM J. Numer. Anal. **55** (2017), no. 2, 1024–1056.
[48] ———, *Fourth- and higher-order interface tracking via mapping and adjusting regular semi-analytic sets represented by cubic splines*, SIAM J. Sci. Comput. **40** (2018), A3755–A3788.
[49] Q. Zhang and A. Fogelson, *MARS: An analytic framework of interface tracking via mapping and adjusting regular semi-algebraic sets*, SIAM J. Numer. Anal. **54** (2016), 530–560.

(Qinghai Zhang) CORRESPONDING AUTHOR
Current address, Qinghai Zhang and Zixuan Li: School of Mathematical Sciences, Zhejiang University, 38 Zheda Road, Hangzhou, Zhejiang Province, 310027 China
Email address, Qinghai Zhang: qinghai@zju.edu.cn